3-D seismic stratigraphic inversion applied toan oilfield offshore of Angola

Francisco da Cunha, Sonogol
Fernando Moraes, Uenf
Paul Johann, Petrobras

Abstract

The integration of well log data, poststack 3-D seismic data and conceptual geological knowledge (structural and stratigraphic) provides accurate information for reservoir modeling and improve the implementation of efficient well developments planning.

Stratigraphic deconvolution aims at improving the resolution which is here of paramount importance (Brac et al, 1988). Seismic data gives indirect three-dimensional information about the reservoir properties that can be integrated with well log derived information.

For seismic inversion approach the key wells from the area of study, were sonic and neutron-density log, were edited and processed through careful petrophysical analysis. Geological markers near and at the reservoir levels for these wells were also interpreted to calibrate the regional seismic interpretation.

The stratigraphic seismic inversion consists of calibrating to tie key geological intervals from the wells with the seismic horizons to build a 3-D initial model, and finally going through the inversion procedure to match seismic amplitudes by updating the acoustic impedance model.

The initial model, an 3-D acoustic impedance model, is buiding from the interpolation of well log information. The inversion methodology is carried out in an time window. We use the trace amplitudes as the constraints. The initial acoustic impedance model is modified through an iterative procedure until the seismic synthetics volume generated from the updated model match the real seismic data. The end product of the inversion procedure is a 3-D inverted acoustic impedance and associated reflectivity volumes.

Introduction

This methodology will be illustrated on an field discovered in a water depth of approximately 600m, within the Lower Congo Basin, offshore of Angola, encompassing a Tertiary clastics of the Malembo Formation setting. The field lies in elongate trending regional growth fault. The hydrocarbon bearing occur on the hanging wall flank of this growth faulting,

The wells have tested Upper to Middle Miocene, encountering biodegraded oil and shows gas. The sand reservoir sequences consisting of relatively thin layers are very porous and permeable.

The main reservoirs objectives are the deltaic sands of the Middle and Upper Miocene turbiditic. The seal is supported by major rollover growth faulting, by dip and an thick marine clay (Top Miocene regional overlying the RS3T horizon).

The structure of the field in study complex model is fairly typical of marine passive margin successions, which tectonic and sedimentary evolution is closely linked to the Neocomian breakup of Gondwana and subsequent opening of the South Atlantic Ocean. The stratigraphic column is a classical rift/drift sequence. The field in study is located in one series of late Tertiary depot throughs within the Miocene thick, and is controlled by rollover into a westerly hading growth faulting, which defines the eastern limit of the field.

The complex depositional system represent fully marine environment, probably in a distal shelf to upper bathyal setting a base of slope comprising a series of sand having been deposited during turbiditic discharges from the shelf generating different reservoir sand levels in the depth

This project is largely based on the 3-D seismic data, covering about 231 Km², with emphasis placed on the preservation of true amplitudes. Data quality shows some amplitude distorsion and poor quality where occur a conjuction of pull-down and absorption effects. Structural control from seismic interpretation is good along the field. For this instance, decided to pick the fault pattern after inversion the data. Vertical and lateral sand distribution vary widely in the eastern and northern flanks of the field. Seismic resolution is low due presence of extremely high amplitudes in the gas cap zone

The wells used for calibration are posted on the map, the southern PG-1 well and the northern PG-2 deviated well with two side-track. Despite the sand/shale impedance contrast, the amplitude map obtained by extracting amplitudes along the determined layering, image clearly seismic facies separation between PG-1 and PG-2.

The main sources of uncertainty come from the net/gross ratio, the variability of petrophysical properties and the OWC and GOC location.

The objective of the study presented here is to show a particular methodology for using integrated tools in cases where the amount of well information is sparse in order

- to identify the internal reservoir architecture of the field
- better to characterize fluid contacts locations
- to evaluate the possible existence of communication or not at reservoir levels between the wells PG-1 and PG-2
- to create numerical model to allow the comparison of alternative field development scenarios and revise the reserves estimate for to remove the risk associated at the field development.

Principles of the methodology

In order to achieve the proposed objectives, the project was approached in four part effort. First, a partial data inventory was made for the area of study. The purpose of the inventory was to determine all subsurface data available including log, core, core analysis data, VSP, checkshot survey, for the wells and 3D seismic data. Secondly, well logs were formatted in software SAS, and then loaded in Easytrace for editing, processing and modeling 1D. Synthetic seismograms were generated for each well in order to correlate well to seismic. For the synthetic seismogram generation in Easytrace, the wirelines logs were transformed from depth to time domain, followed the extraction of an precise source wavelet at each well which, when convolved with the reflectivity series, generates synthetic trace. By average of the all wavelets generated, have produced a single best wavelet representative. Four seismic horizons were roughly conducted to provide the time window (top & base of the reservoir, more two internal control horizons), structural architecture of the field and to serve as initial model for the process of the inversion. Thirdly, by accounting for seismic amplitudes, seismic interpretation, petrophysical data and geologic knowledge we were able to generate inverted volume of acoustic impedance. And finally, the inverted volume were integrated, and the horizon and fault interpretation were refined based on the inversion results. Based on local petrophysical relationships and geostatistical approaches, porosity variations could be estimated from acoustic impedance layers, and porosity maps produced for each reservoir interval. A geologic modeling was generated as input for the location of the new well planning.

Conclusions

Acoustic impedance interpretation provides better indication of reservoir distribution than conventional seismic data, even thin reservoir sands. The seismic stratigraphic inversion adds substantial information to the original seismic data and to refine the drilling planning of the new wells.

The results demonstrate a clear potential for use of the integrated system, coupled with a wireline well, seismic, core. Major advantages of this methodology are that it is conclusive and it provides detailed image of trhe reservoir.

Recommendations

Further study should be cconducted to explore the full capabilities of this methodology it may be accepted for use by several utilities in reservoir modeling. Possible limitations include application for poor reservoir conditions.

Acknowledgements

The authors wish to thank the Sonangol, Petrobras and Uenf for permission to publish this work

Bibliography

Johann, P., 1997, “Inversion sismostratigraphique et simulations stochastiques en 3-D”. Ph.D Thesis, Paris VI (Pierre et Marie Curie).

Johann, P., 1999, “Seismic Geoinversion as a Horizontal Well Positioning Tool: Applications in the Marlim and Barracuda Fields, Deep-Water Campos Basin”.

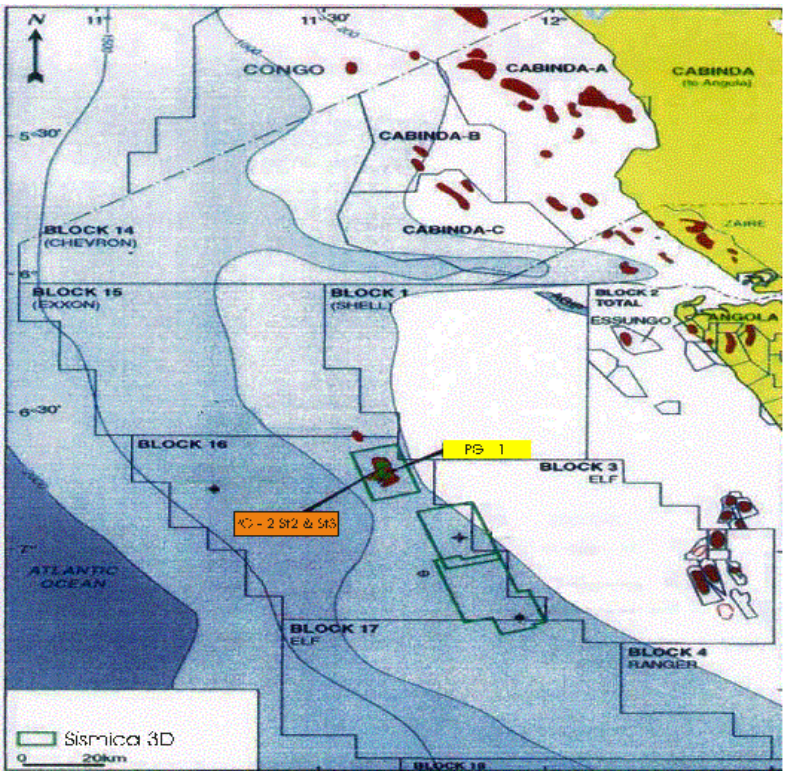

Figure 1 – Angola offshore blocks localization map.

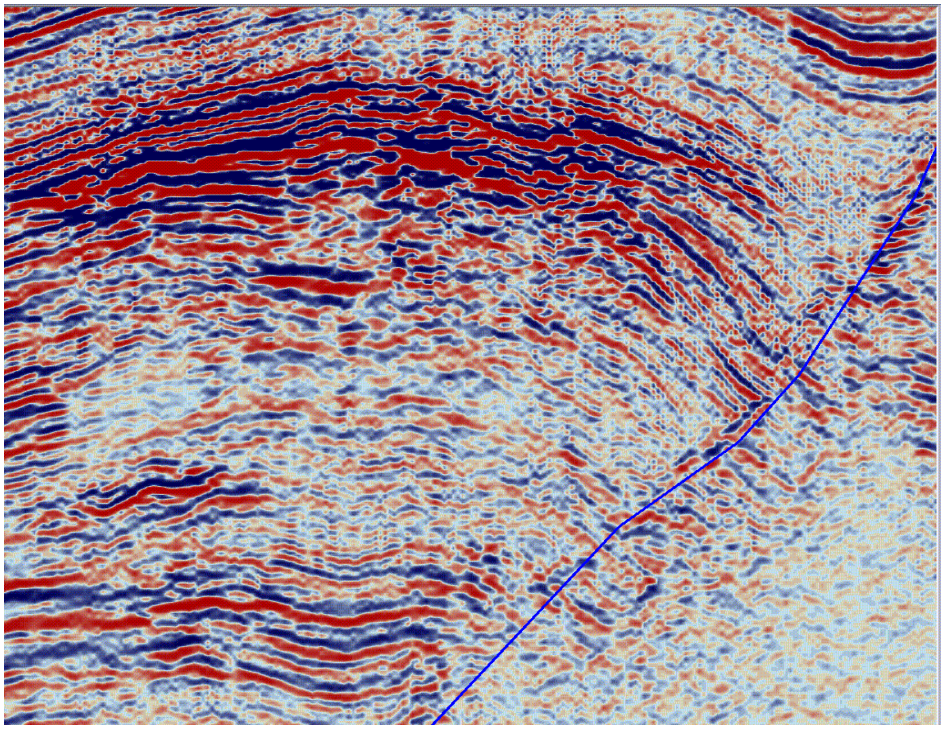

Figure 2 – Amplitude section with structural and stratigraphic framework of Angola offshore reservoir

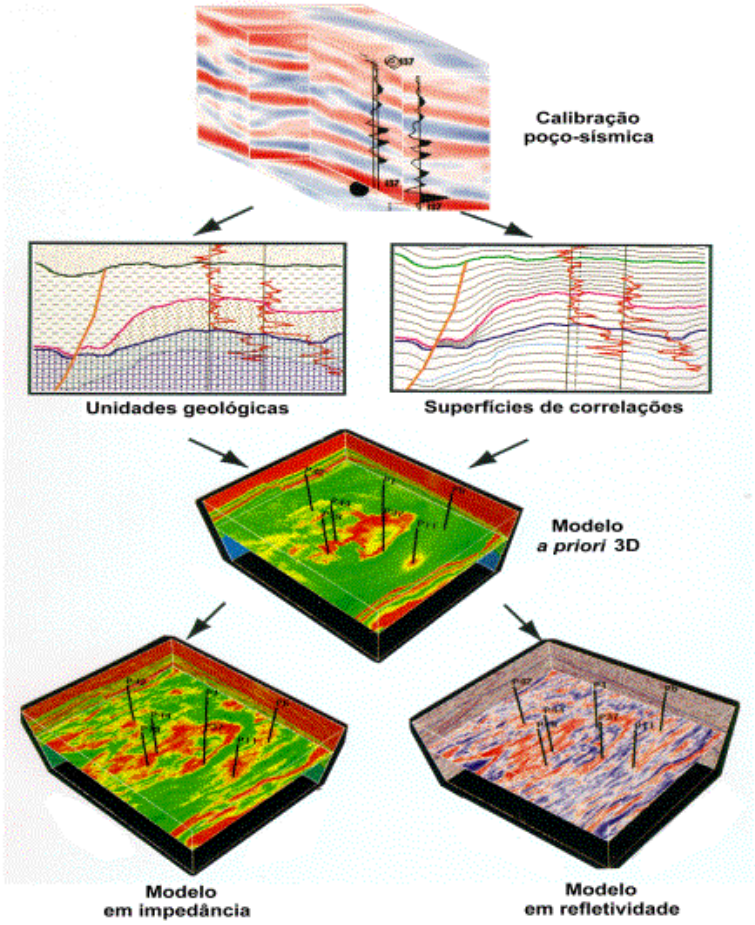

Figure 3 – 3-D stratigraphic inversion methodology.

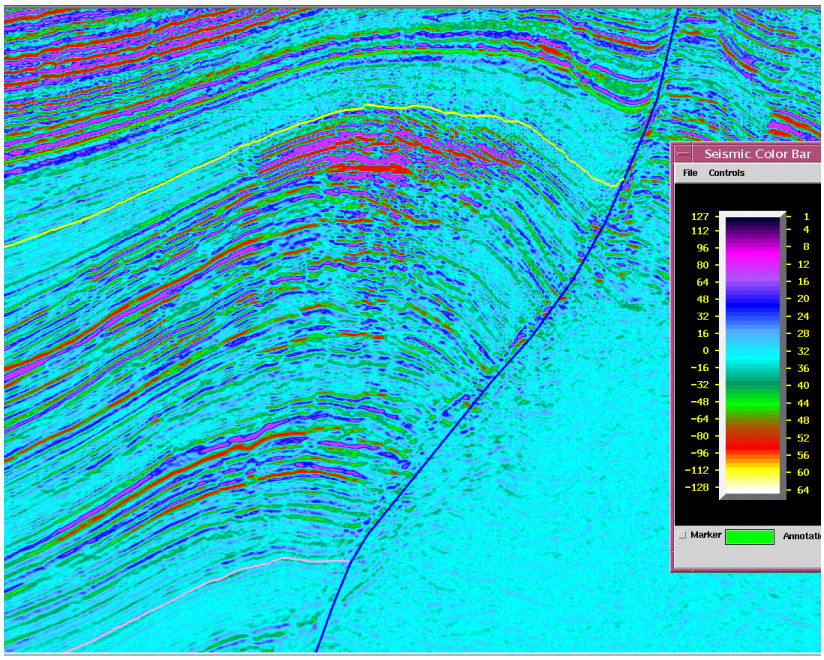

Figura 4 – Acoustic impedance after stratigraphic inversion.

A simple and effective method to extrapolate sonic profiles to the surface

José Adauto de Souza

Petrobras SA

ABSTRACT

The extrapolation of sonic profiles in oil industry is a routine for the geophysicists. A good correlation between geological data in wells and seismic reflectors in a seismic line is necessary to reach good results in oil prospection. If a VSP(Vertical Seismic Profile) is available nearby an exploratory or development well, this routine becomes easy. Commonly the only available information is the sonic log, which in general doesn't starts at the surface. So, the geophysicist begins compiling and integrating technical data from different sources: seismic velocities, geological information, velocity surveys, regional velocity pattern, sonic profiles, etc. Even after a good job, the definition of a velocity to extrapolate sonic data to surface is not an easy task. One usual decision is to use the interval velocity at the beginning of the sonic profile as the interval velocity up to the surface.

In this paper is proposed a simple and effective method to extrapolate sonic profiles: basically it is an interactive computer based application where the user may decide which velocity is good to do this extrapolation. The application creates and integrates velocities starting from the surface that rise exponentially and reach the beginning of sonic profile, then starts integrating the sonic profile. Visually the user may decide: the velocity used to extrapolate is too high, too low or good enough. If this velocity is not good, a visual inspection makes clear that the velocity gradient of the extrapolation doesn't fit the velocity gradient at the beginning of the integrated sonic profile.

INTRODUCTION

One way to compute TxD (time x depth) curves is to use the data from the sonic profile. The sonic time integration and extrapolation gives a complete relation of time with depth, and it may be written as:

$$T(Z) = \sum_{Z=1}^{S-1} 1/Ve + \sum_{Z=S}^{F} 1/Vs \,, \qquad (1)$$

where T(Z) = time as a function of depth
Ve = extrapolation velocity
Vs = sonic velocity
S = initial depth of sonic
F = final depth of sonic

The key to solve equation (1) is to decide a good value to be used as Ve. Approximated values may be obtained mainly after some interpretation of technical information found in velocity surveys, seismic data, geology and regional velocity pattern of sedimentary layers. Sometimes the definition of Ve is not easy and a bad definition may imply a complete failure of a petroleum industry project. Also, a project can be discarded as no economic when in reality it is economic. Recently, in our company we had an example of this type of situation. An old standby project became attractive due to changes in gas/oil demand and we

start a new evaluation. The planning was to drill a wildcat in a new structure nearby an oil/gas field, based on seismic lines. There are no seismic lines over the oil/gas field, due to geographical and environmental constraints. So, the conversion of depths of field wells to time is basic to estimate gas/oil and oil/water contacts in the planned wildcat. At the end we concluded that the project was not attractive due to changes in net-pay, total area and fluid percentage: the project became an oil project and not a gas project, as anticipated in the old evaluation. Mainly those changes were due to a new interpretation of sonic extrapolation velocity of wells from the oil/gas field.

THE METHOD

The velocity gradient of geological layers has an exponential decay with depth: velocities change more rapidly at shallower depths. The use of a constant velocity (Ve) to extrapolate the sonic log disagrees with this property. This disagreement doesn't imply in failures, if Ve is good enough and considering that the target zones as a general rule are below the beginning depth of the sonic profile. Why not to use this property (gradient with a exponential decay) to solve for Ve? The method presented here use this property and give us a nice chance to compute the extrapolation velocity. Basically, it builds a velocity curve starting from a user given value at the surface and an ending value at the beginning depth of sonic survey, rising exponentially. After this, the velocity sonic values are integrated to complete the TxD curve. The complete integration may be written as:

$$T(Z) = \sum_{Z=1}^{S-1} 1/Vi + \sum_{Z=S}^{F} 1/Vs, \qquad (2)$$

$$Vi(Z) = V0*EXP(cZ), \qquad (3)$$

$$Vf(S) = \left\{ \sum_{Z=1}^{S-1} Vi(Z) \right\} / (S-1), \qquad (4)$$

where T(Z) = time as a function of depth
Vi(Z) = interval velocity in the extrapolation zone (computed by application)
Vf(S) = average extrapolation velocity at depth S-1(user defined)
V0 = velocity at surface (user defined)
c = constant value (computed by application)
Z = actual depth
Vs = sonic interval velocity
S = initial depth of sonic
F = final depth of sonic
EXP = exponential with neper constant e

The constant c is computed by doing computer iterations. The definition of an initial value to be V0 is not important, only it must be lower than the average velocity Vf at the end of the extrapolation zone. It is common to use 1500 m/s for Tertiary basins and 2000 m/s for Lower Cretaceous basins as V0 value. Vf must be higher than V0 and this value is obtained after some interactive actions between the user and a Pc (personal computer) graphic application based on equations (2), (3) and (4). The user defines Vf visually, when the extrapolated velocity gradient is similar to the integrated velocity gradient at the beginning of the sonic profile. This will not work very well if the lithology in the extrapolated zone has a velocity gradient completely different compared with the velocity gradient present at the beginning of the zone covered by the sonic. One example of this occurs when the well has clastic sediments in the extrapolated zone and limestones immediately below.

Figure 1 presents an output graphic image of an integrated and extrapolated sonic profile. The green curve was computed extrapolating a velocity function from V0 = 1800 m/s to Vf = 2000 m/s, till the magenta rectangle close to 200 ms and 200 m (x,y). The magenta rectangle gives the position where the sonic profile starts. Nearby this position there is a blue straight line that represents the velocity gradient at the beginning of the sonic profile. Clearly this blue line is moving away from the green line, which means that the velocity

gradient defined by the velocity Vf at the end of the extrapolation is different if compared with the gradient of the sonic. Similarly, **figure 2** shows that the blue line is parallel to the green line: the extrapolated gradient is close to the sonic gradient (Vf=2440 m/s). **Figure 3** shows another curve with Vf=3000 m/s and is easy to interpret that the blue straight line is crossing the green curve: in this case the velocity gradient in the extrapolated zone is smaller than that of the sonic profile.

So, we may summarize:

a) A Vf lower than the average velocity at the beginning of the sonic produces an image where the blue curve moves away from the green curve(**figure 1**). Vf may be interpreted as lower than the good one.
b) A Vf higher than the average velocity at the beginning of the sonic produces an image where the blue curve crosses the green curve(**figure 3**). Vf may be interpreted as higher than the good one.
c) A Vf close to the average velocity at the beginning of the sonic produces an image where the blue curve is quite parallel to the green curve(**figure 2**). Vf may be interpreted as being a good velocity to extrapolate the sonic curve.

It is important to mention that the visual selection to define Vf is sensible to changes of 10 m/s, meaning this definition is quite precise.

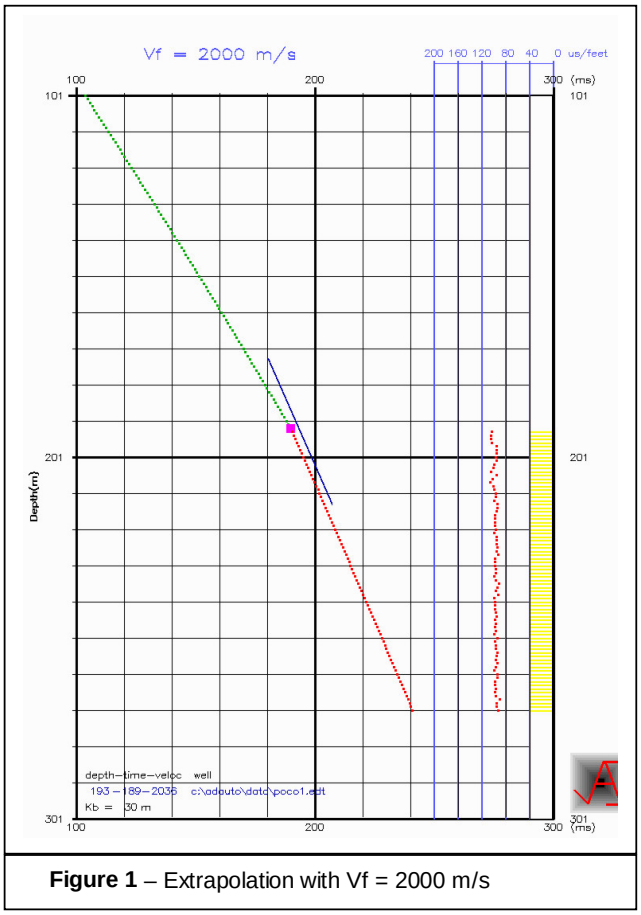

Figure 1 – Extrapolation with Vf = 2000 m/s

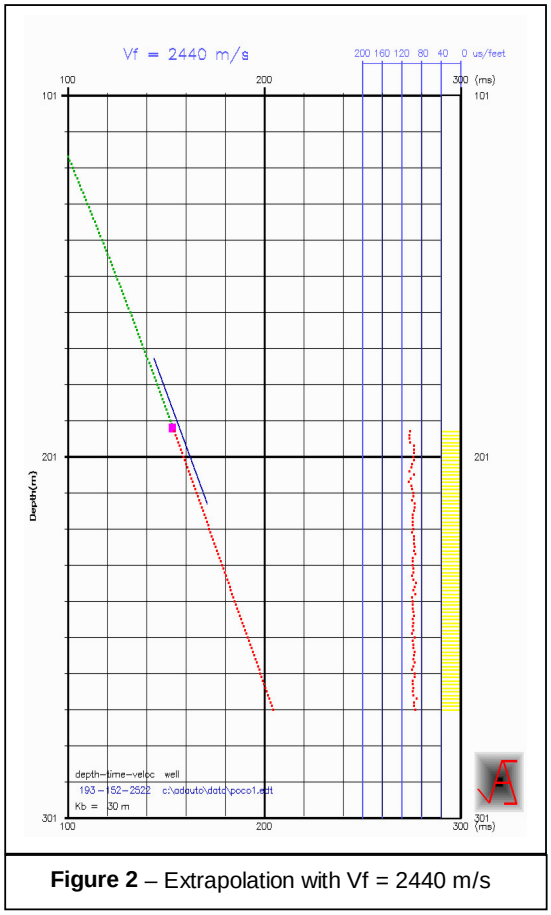

Figure 2 – Extrapolation with Vf = 2440 m/s

Figure 4 presents a final interactive result (complete well) where the interpreter has defined an extrapolation average velocity Vf. In the right hand part of the figure a red curve represents the sonic readings and a colored column represents the lithologies. In the left two curves can be seen: the magenta (average velocities) and the red (interval velocities). In the same figure the green line (TxD extrapolated and integrated) has good fit with some blue boxes, that are data from a VSP survey. An additional output of the computer application is a columnar ASCII file including depths, two-way times, average velocities and interval velocities of the well.

CONCLUSIONS

A simple and effective method to extrapolate sonic curves to surface has been presented. Basically, it solves the problem using the velocity gradient of the geological layers. An exponential decay curve is used to compute and integrate a complete set of interval velocities along the extrapolation zone, where the sonic has no readings. The method is sensitive to variations of 10 m/s in the computation of the extrapolation velocity, what means that it is very precise. A velocity mistake of 10 m/s in a extrapolated zone of 300 m using 2000 m/s as Vf introduces one error of 1.5 ms or 1.5 m. In the example showed in the figures, the average velocity in the first 15 m covered by the sonic is 2959 m/s (depths 224 to 238 m). If the interpreter decides to use this velocity as the one to extrapolate the sonic (Vf), an error of 27 ms will be introduced, assuming that the velocity 2440 m/s is the correct one. You may do some immediate guesses if the length of the extrapolation zone is higher ant the velocities are lower: the error introduced rises rapidly to values higher than 50 ms.

The interpreter must be careful when lithologies in the extrapolation zone are quite different compared with the lithologies in the beginning of the sonic survey: this may result in velocity gradients quite different and the method may not work very well. Anyway, in this case, the method still gives a chance to compute the extrapolation velocity by using additional geological and geophysical information.

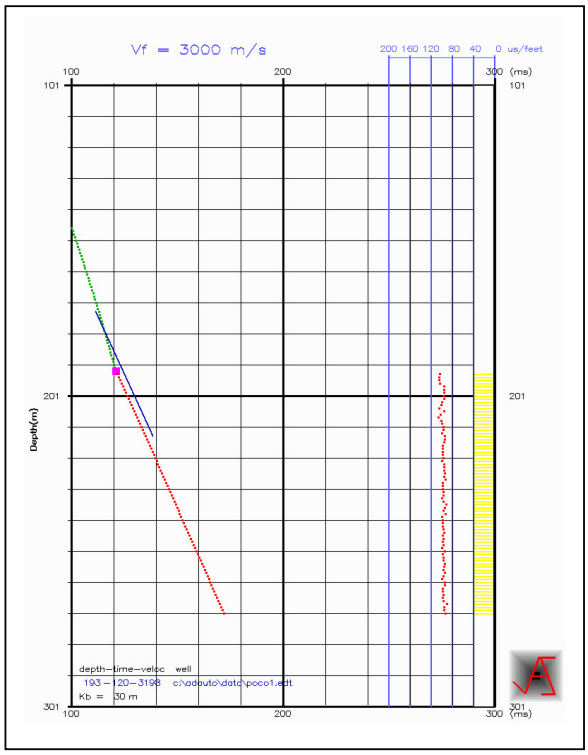

Figure 3 – extrapolation with Vf = 3000 m/s m/s

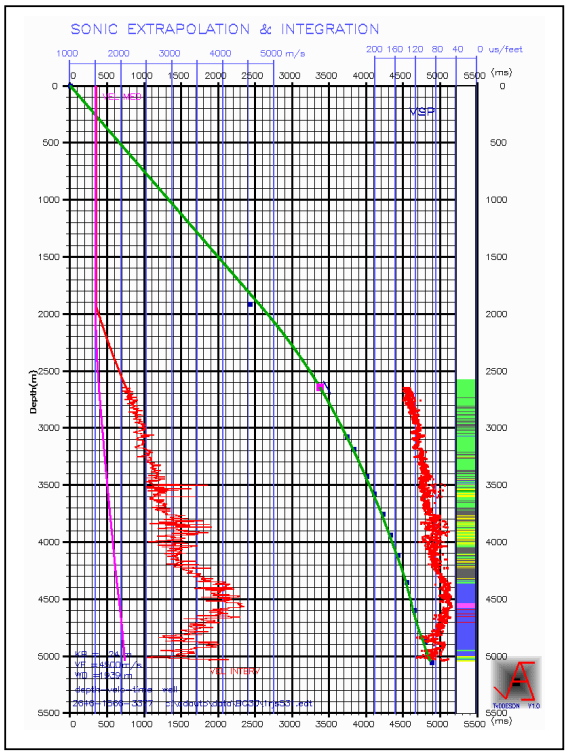

Figure 4 – final graphic output

REFERENCES

- Duarte, O. O.,1997, Dicionário Enciclopédico Inglês-Português de Geofísica e Geologia, Sociedade Brasileira de Geofísica, 304 p.

ACKNOWLEDGMENTS

I would like to thank Petrobras for permission to present and publish this work.

Aplicação da Coerência Sísmica à Detecção de Feições Estratigráficas e Estruturais

Raul Dias Damasceno, PETROBRAS S.A., Brasil; Adelson Santos de Oliveira, PETROBRAS S.A., Brasil, André Gerhard, Brasil; Amin Bassrei, IF-CPGG-UFBA

Abstract

Seismic coherence, defined as the phase relationship maintenance through a set of reflectors, can be used as an auxiliary tool in order to map stratigraphic and structural seismic features. In this paper, the results of some coherence methods based on semblance, eiggenstructure, and shaping filters are showed. Each method was applied to real and synthetic data in order to compare their results in presence of different parameters. An image processing method, named mathematical morphology, was applied on the obtained coherence images in order to improve the continuity of the seismic coherence features. In the conclusion the results are discussed as well as the limitations and recommendations for each method.

Introdução

O conceito de volume de coerência sísmica, introduzido por Bahorich e Farmer (1995), vem despertando cada vez mais interesse, sendo utilizado no mapeamento de feições estratigráficas e estruturais.

No trabalho original de Bahorich e Farmer (1995) a coerência é obtida através da correlação cruzada entre traços vizinhos. Gersztenkorn e Marfurt (1996) apresentam, como evolução de Bahorich e Farmer (1995), métodos baseados em *semblance* e autoestrutura. Nestes, toma-se como base a matriz de covariância dos dados sobre a qual os respectivos algoritmos são aplicados.

Luo *et al.* (1996) apresentou um método no qual a coerência é estimada através da diferença entre traços adjacentes. Mais recentemente, Oliveira (1999), apresentou um método onde a coerência é obtida através da diferença quadrática entre filtros conformadores calculados entre traços sísmicos adjacentes. Neste trabalho, apresentamos o resultado parcial de experimentos realizados envolvendo os métodos citados, onde foram avaliadas as respostas destes frente à variação de diversos atributos, como deslocamento vertical, variação de freqüência e conteúdo de ruído aleatório dos dados.

Análise e comparação dos métodos

A coerência é uma medida matemática da similaridade. Quando aplicada aos dados sísmicos fornece um indicador da continuidade entre dois ou mais traços previamente janelados. Idealmente, o grau da continuidade sísmica é um indicador direto da continuidade geológica. Quando aplicada ao delineamento de feições estratigráficas e estruturais, a coerência tem obtido melhores resultados em dados tridimensionais migrados em tempo ou profundidade, embora possa ter aplicação em qualquer etapa do processamento.

A análise e comparação entre os métodos foram realizadas a partir da aplicação a dados sintéticos e reais, frente a diversos atributos, como variação de freqüência, fase, amplitude, bem como em situações geológicas distintas, como diferentes ângulos de mergulho e rejeito de falhas.

Dois tipos de traços foram utilizados na geração dos dados sintéticos, um pulso tipo Gabor e cossenóides. Esta escolha foi feita em razão dos métodos não serem lineares, portanto o que acontece com um pulso não é a soma do que acontece com suas componentes de Fourier. Como o dado real não é nem um pulso, nem uma cossenóide, procurou-se ter uma visão global do comportamento dos métodos baseada em seus extremos. Como unidade de medida padrão utilizaram-se os períodos dominantes, permitindo assim a extensão dos resultados obtidos aos dados reais a partir do conhecimento das freqüências contidas nestes. Os testes numéricos, bem como resultados analíticos, mostraram que os resultados obtidos são dependentes de diversas variáveis como o tamanho da janela em relação ao período, nível de ruído, fase entre a janela e os dados, variação de amplitude, deslocamento vertical (rejeito) e do relacionamento entre estas.

Deslocamentos verticais entre sinais de traços sísmicos vizinhos são descontinuidades comuns, sendo indicativas principalmente de falhamentos. Se imaginarmos o deslocamento vertical como sendo dado por uma mudança de fase, outras estruturas podem ser englobadas nesta análise como canais, recifes, etc. Estas diferenças de fase entre traços vizinhos mostraram-se como o principal fator de sensibilização dos métodos. Considerando a relação entre o deslocamento vertical e o tamanho da janela, sendo ambas as grandezas dadas em percentual do período, a pesquisa mostrou que para os métodos de diferenças, filtro conformador e *semblance* a melhor resposta ocorre quando o deslocamento é máximo, ou seja, para uma diferença de fase de π. Já o método autoestrutura apresenta seu maior desempenho para deslocamentos de $\pi/2$, apresentando um mínimo em π (vide Figuras

1 a 4). Este resultado é vantajoso em relação aos demais métodos, visto que a faixa de melhor desempenho é atingida mais rapidamente. A resolução vertical da resposta a ser obtida está diretamente relacionada ao tamanho da janela utilizada. O tamanho ideal de janela é de um período dominante, embora somente o método autoestrutura tenha se mostrado restritivo a valores menores, de modo que a menor freqüência dominante balizará o tamanho da janela a ser utilizada.

Os métodos são bastante sensíveis, sendo possível mapearem-se pequenas descontinuidades da ordem de décimos do período. Fatores limitantes ao desempenho são os níveis de ruído aleatório e o mergulho.

O nível de ruído mostrou -se o ponto de maior sensibilidade, principalmente em relação ao método do filtro conformador. Nesta situação, o método de autoestruturas apresenta o melhor desempenho, fato que pode explicar os ótimos resultados registrados pela literatura. Tal fato recomenda um tratamento acurado dos dados de modo a torná-los os mais livres possíveis de ruídos principalmente no caso do conformador. As Figuras 7 e 8 comparam a aplicação do método do filtro conformador a dados com e sem uma filtragem FX respectivamente. A Figura 9 mostra a mesma imagem obtida com o método *semblance* sobre dados com filtragem FX.

As limitações impostas pelo mergulho devem-se ao fato da busca de coerência ocorrer no sentido horizontal de modo que as mudanças amostra a amostra, passam a ser vistas como descontinuidades. Para os métodos de autoestrutura, diferenças e *semblance* é necessário uma busca do valor e direção de mergulho previamente à aplicação dos métodos. Esta busca implica em um maior esforço computacional, além da introdução de imprecisões surgidas do processo de interpolação. No caso do filtro conformador um incremento de mergulho constante traço a traço implica em filtros formados por pulsos com deslocamentos iguais em relação ao *lag* zero, ou seja, já incorporando o efeito de mergulho. Os testes mostraram que a presença de mergulho exerce uma forte influência sobre os métodos de diferenças e autoestruturas, e em menor escala sobre o método *semblance*. O método do filtro conformador, devido a sua metodologia, é praticamente imune ao mergulho.

Outros parâmetros que influenciam o desempenho dos métodos são a variação de amplitude e a fase dos dados em relação à janela. A fase em relação à janela é um parâmetro que mostrou pouca importância podendo ser negligenciado. Já a variação de amplitude influi de forma direta no caso dos métodos autoestrutura, conformador e diferenças e inversa no caso do *semblance.*

Tratamento das imagens

O caráter policromático dos dados sísmicos faz com que a resposta dos métodos não seja uniforme em toda a seção fazendo com que as estruturas mapeadas apresentem lacunas na imagem gerada. Visando obter uma imagem de melhor qualidade, através do preenchimento de tais lacunas, aplicou-se um método cujo princípio se baseia na teoria da morfologia matemática (Serra, 1975), cujo princípio é a descrição da imagem como regiões ou conjuntos. Os operadores são construídos pela combinação de operações elementares como união, intersecção e operações de composição. Estes operadores e as operações da Morfologia matemática são ferramentas para extração de informações das imagens. As Figuras 5 e 6 ilustram a aplicação da morfologia matemática, mais especificamente do operador de fechamento.

Conclusões

Em razão dos resultados obtidos utilizando-se traços gerados por um pulso Gabor e por cossenóides terem sido compatíveis, podemos estender o comportamento observado nos testes aos dados reais. Todos os métodos mostraram bons resultados e grande capacidade de detecção. Os métodos diferença vetorial e filtro conformador são mais sensíveis a pequenas variações sendo, portanto também mais susceptíveis ao ruído aleatório. O método autoestrutura apresentou os melhores resultados, sendo mais eficiente em presença de ruídos. Em termos de procedimentos de rotina, os métodos *semblance* e diferenças vetoriais são mais rápidos, podendo ser utilizados em uma abordagem mais expedita que exija menor precisão. Já o método baseado em filtros conformadores, embora apresente a vantagem de não depender dos mergulhos, não apresentou imagens tão nítidas quanto os demais, fato que pode ser atribuído a utilização de um menor número de traços. A aplicação da morfologia matemática mostrou-se como uma ferramenta eficaz, permitindo a recomposição de estruturas apenas parcialmente mapeadas pelos métodos de detecção.

Referências

Bahorich, M. e Farmer, S. (1995) 3-d seismic discon tinuity for faults and stratigraphic features: The Coherence cube, The Leading Edge, **10**:1053-1058

Gesztenkorn, A. e Marfurt, K. J. (1996) 3-d seismic discontinuity for faults and stratigraphic, 66th Ann. Internat. Mtg., Society of Exploration Geophysicists, Expanded Abstracts, INT.2.2, **1**:328-331.

Luo, Y.; Higgs, W. e Kowalik, W. (1996) Edge detec tion and stratigraphic analysis using 3d seismic data, 66th Ann. Internat. Mtg., Society of Explora

tion Geophysicists, Expanded Abstracts, INT.2.1, **1**:324-327.

Oliveira, A. (1999) Shaping filters as a tool for edge detection, VI Congresso Internacional da Socieda de Brasileira de Geofísica. Em CDROM.

Serra, J. (1982) Image Analysis and Mathematical Morphology. Academic Press.

Agradecimentos

Gostaríamos de agradecer a PETROBRAS pela oportunidade de desenvolver e publicar este trabalho.

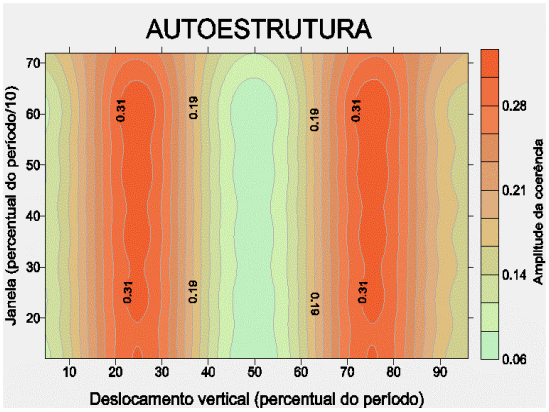

Figura 1

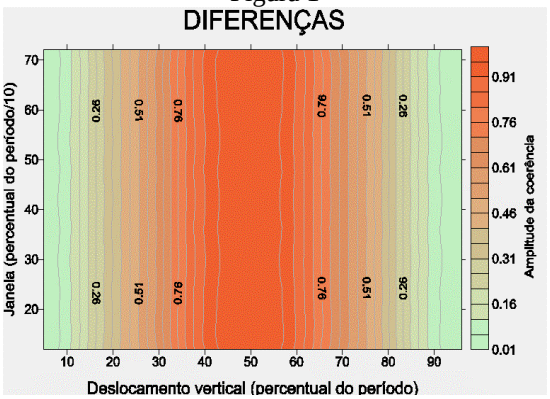

Figura 2

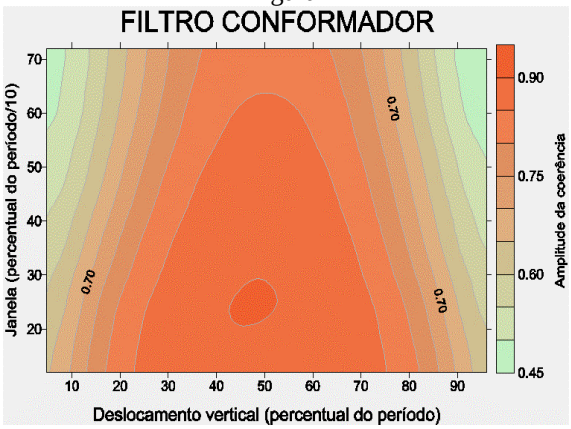

Figura 3

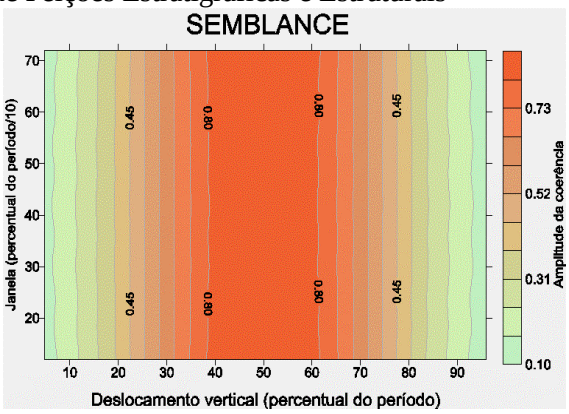

Figura 4

Figuras 1 a 4 - Resposta dos métodos considerando a relação deslocamento vertical (rejeito) x comprimento da janela, ambos medidos em percentual do período da janela.

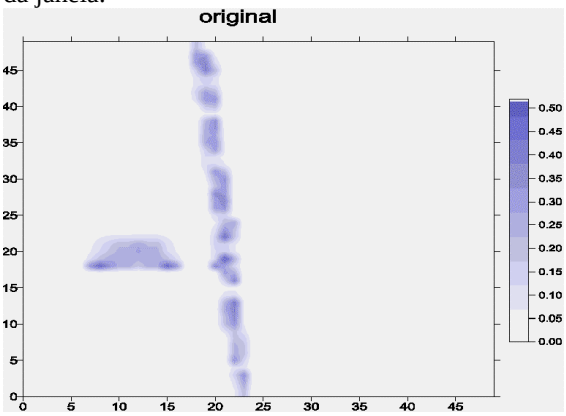

Figura 5

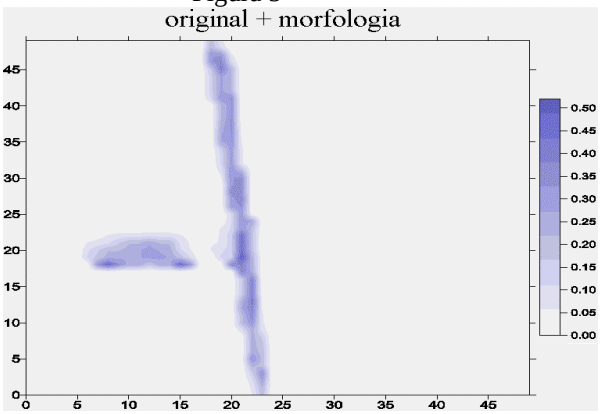

Figura 6

Figura 5 e 6 - Aplicação da morfologia matemática: Observar que as lacunas existentes na falha da Figura 5 foram suprimidas na figura 6.

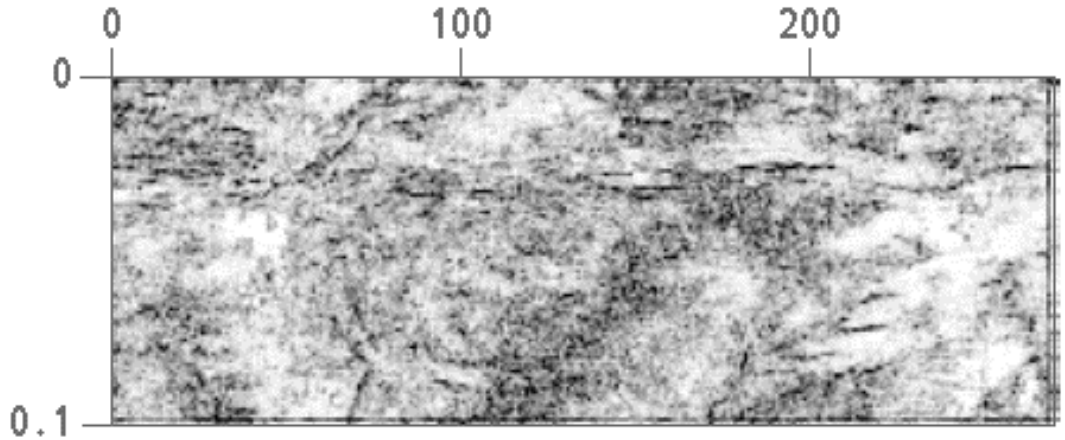

Figura 7 - Aplicação do método do filtro conformador.

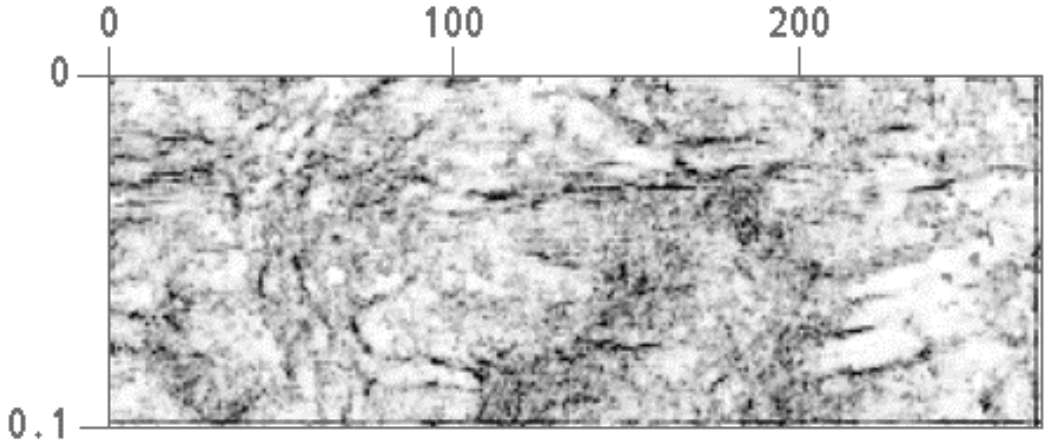

Figura 8 - Idem da Figura 7, mas sobre dados onde foi aplicada previamente uma filtragem FX.

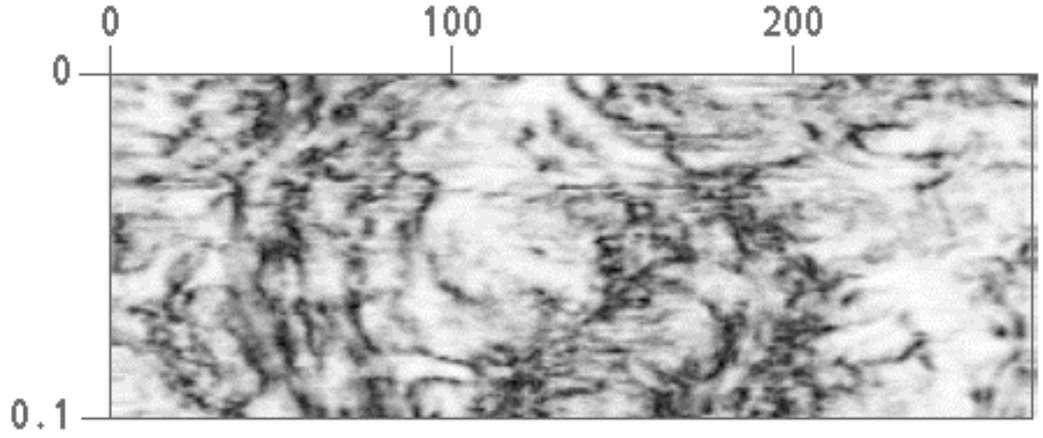

Figura 9 - Aplicação do método *Semblance* sobre os dados utilizados na Figura 8.

Borehole Seismic for imaging below surface basalt in Volcán Auca Mahuida Field, Neuquén basin, Argentina.

Luis Pianelli, Repsol-YPF, Argentina
Emilio Sanchez Repsol-YPF, Argentina
Andres Vottero Repsol-YPF, Argentina
Eduardo Corti, Schlumberger, Argentina
Flavia Croce, Schlumberger, Argentina

Abstract
Surface seismic response in volcanic areas covered by basaltic layers usually shows a very poor seismic image. This fact makes it difficult to find new well locations based on surface seismic information.
In Neuquén province, in the west of Argentina, a borehole seismic solution was tested: Offsets VSP were run to get seismic images below the basalt on surface.
The project was established in two steps. The first one was to run a VSP to verify, with quick processing at the well site, that there was actually enough energy reflecting on target layers, and coming back as upgoing reflections to the receivers in the well. If this is verified then the different offsets will be acquired.
This case history shows a successful example of how borehole seismic can help in providing seismic images due to its differences in source and receivers setups compared with surface seismic.
The survey was designed to get images in three different azimuths. Acquisition parameters were defined after performing the raytracing modeling.
This modeling allowed us to define receiver and source positions in order to verify the lateral coverage. Due to the complexity of the surface some sources locations had to be relocated according of the raytracing modeling.
The processing was done for each set of data generating images through GRT migration. The velocity model used by the migration was updated by the first arrival travel times from the VSP data.
Images have shown very good quality reflectors in contrast with the results of surface seismic. This allowed us to perform a seismic interpretation on a workstation and create a final map.

Introduction

The oil reservoir Volcán Auca Mahuida is located in the north side of the homonym volcano, in the province of Neuquén, República Argentina (Fig1).
The sedimentary column, in this sector of the Neuquina basin can reach 5000 m of thickness, with a remarkable wedge out in northeast direction, toward the basin border. At regional level is defined a great structure, coincident with the Volcán Auca Mahuida, possibly generated starting from the intrusion of igneous bodies (vein, layer and domes) in Quintuco formation, Vaca Muerta.

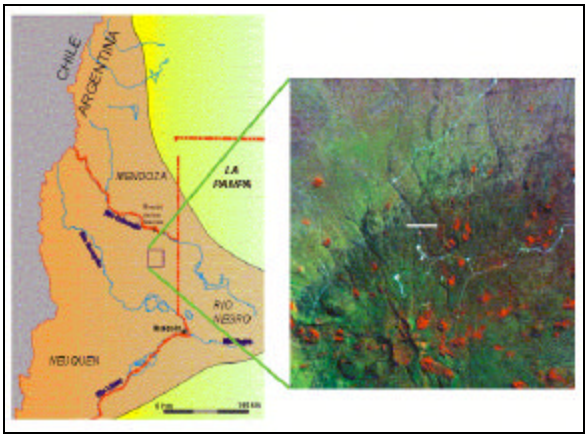

Figure 1 – Area Location

The reservoir levels are represented by Centenario and Mulichinco Fm., to a variable depth according to the topographical conditions among the 2500 and 2900 mbbp and for the same intrusive bodies, to depths up to 3500 mbbp.
The biggest perspectives are centered in Mulichinco Fm (150 m of thickness) whose sandy packages, of possible fluvial ephemeral distal genesis, possess excellent reservoir conditions (porosity: 18-20%, permeability: 50-500 md). Sandy-calcareous levels interpreted as transgressive events, that would act as seals controlling the vertical diffusion of the hydrocarbons, limit these sandy bodies.
A basaltic cover between 200 and 400 m of thickness it covers the area almost for complete, hindering the surface operations.
The seismic lines registered in different times and with different technologies have not been able to save this inconvenience. The quality goes falling as the basalt thickness is increased until the total loss of information in the location area. The little reliability of the seismic isocronic maps manage to the realization of structural maps using the information offered by the dips of the well logs and the most reliable data of the extreme of seismic lines.
The log data and their correlation suggest very soft dips, of the order of 1-2 deg. On the other hand, the correlation between levels and the contained fluids in

the same ones, in different drillings, indicate unties presence, surely associated to fault systems.
In this way, the maps making with the necessary detail and precision for the development of the area it becomes very complicated, so it was necessary to use a method to obtain a reliable data near the wells area. After analyzing the different technological alternatives available at the present time, with a relationship cost-benefit, it was concluded that the data acquisition with Offset-VSP could be the most effective technique.

Acquisition

The multi-offset VSP requires a thorough preparation to guarantee a practical solution. The terrain conditions may be one of the most important limitations to acquire the data: on one side the lava layer on the surface is a strong reflector, and on the other side the complex topography may make very difficult to locate the source (a vibro) at the ideal positions.
The raytracing modeling provides a valuable information to evaluate the survey, like the lateral coverage and the geometry of the ray-paths (Fig.2).

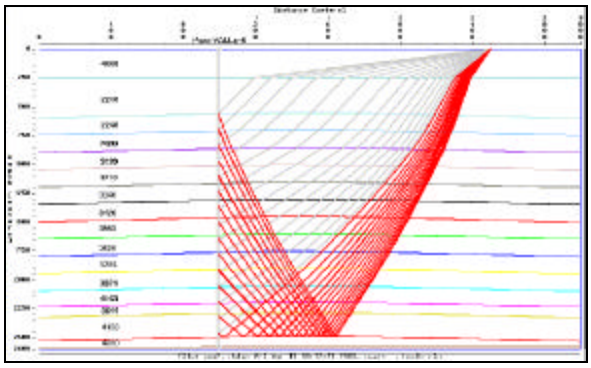

Figure 2 - Ray-tracing Modeling

Sweep parameters were decided based on some tests performed in the area for a surface seismic survey. Large sweep length with large sweep taper windows was selected for this survey.
The interval between levels was selected in order to avoid aliasing of frequencies belonging to the data band with.
The parameters were as follows:
-Acquisition interval: from TD (2350 m) to 1050 m
-Interval between levels: 15m
Source positions (Fig. 3):
-S1= Offset 1928 m, Azimuth 146 deg.
-S2= Offset 1600 m, Azimuth 325 deg.
-S3= Offset 1912 m, Azimuth 108 deg.
Sweep parameters:
-Sweep type: Vibroseis
-Sweep frequencies: 6-50 Hz (lineal)
-Sweep length: 16 sec
-Sweep taper: 1 sec.
Vibro: mertz M18/617, with P.Adv.II
Tool: CSI-A

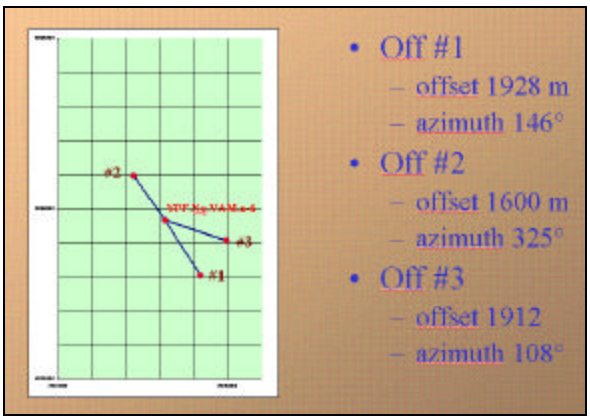

Figure 3 – Well position for each offset

OVSP Processing

A triaxial processing is mandatory in this type of surveys because of the raypath geometry. The three components X,Y,Z, were use to deal with the different angles of incidence and to sparate P wavefields from the total wavefield (P and converted S waves).

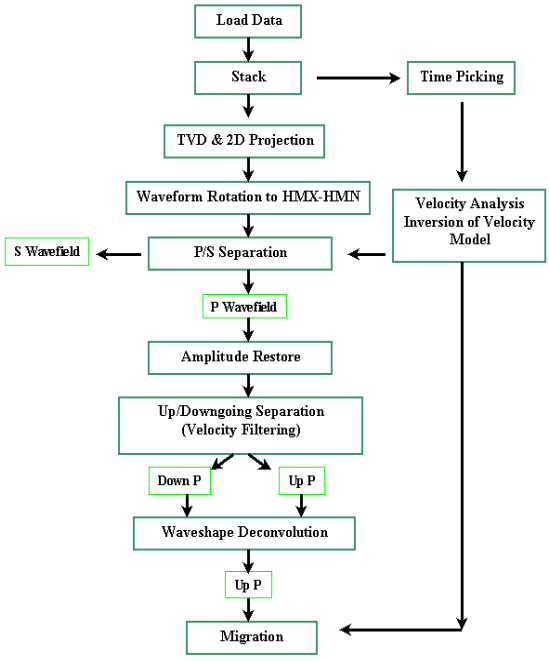

Figure 4 - Processing flow chart

The processing sequence for each source position was (Fig 4):

- Model velocities adjusted by inversion to the VSP first arrival transit times, for each azimuth.
- Triaxial processing: horizontal components HMX (on the incidence plane) and HMN (normal to the incidence plane) were generated from the X, Y and Z components for each offset.
- P and S Wavefield separation.
- Up going and Down going P-waves separation.
- Deconvolution.
- Image generation by migration of Up going P-waves after Dcon., in depth [m] (shown in figure 5) and in time [sec].

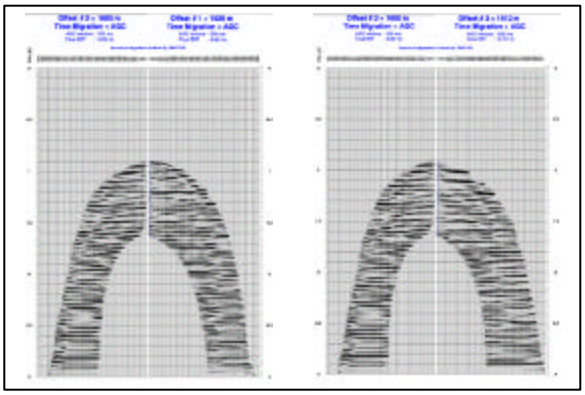

Figure 5 – Migration Image. Offset 2-1 & 2-3.

Well Tie and Interpretation

In figure 6 is shown the tie between the surface seismic image and the OVSP images. It is possible to observe a better quality image in the well seismic results and this was used to improve the interpretation.
Based on this success, many new OVSP surveys were planned and executed, and field development is now being improved by tying the interest horizons. In addition, the geometry of the fault system has being resolved more accurately.
At present the oil reservoir Volcán Auca Mahuida produce 200 cubic meters of oil per day. There are twelve wells drilled, and they were recorded Multi-offset VSP in four of them.

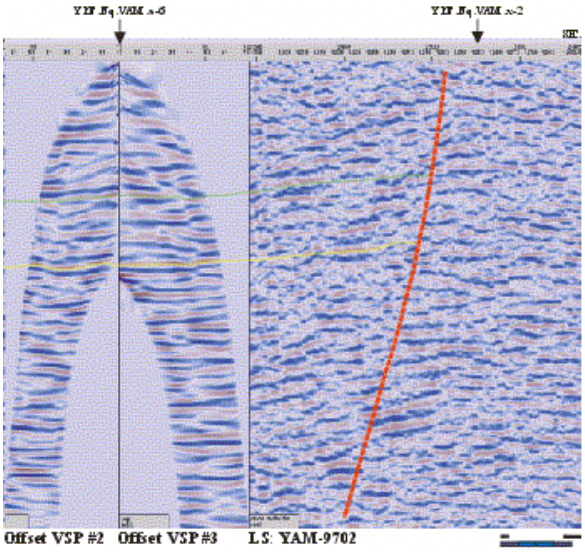

Figure 6 – Offset Image vs. Surface Seismic Image

Conclusions

Multi Offset VSP techniques have been used to improve the seismic image successfully and therefore to improve the interpretation. All these mentioned techniques can be used as a strong aid in locating the best sites for development wells and therefore to reach a better field development.

References

-Cramer, P.W., Reservoir Development Using Offset VSP Techniques in the Denver-Julesburg Basin, Reservoir Geophysics, Edited by R. Sheriff, Investigations in Geophysics N°7, SEG, 1992
-Noble, M.D., Lambert, R.A., Ahmed, H. and Lyons, J., Application of three-Component VSP Data on the Interpretation of the Vulcan Gas Field and Its Impact on Field Development, Reservoir Geophysics, Edited by R. Sheriff, Investigations in Geophysics N°7, SEG, 1992
-Zencich, S., Oil Discovery in the Volcán Auca Mahuida Zone, BIP N°62, June 2000

Acknowledgments

The authors would like to thank Bernardo Moyano and Omar Curetti *(Schlumberger, Argentina)*, Leonardo Rodriguez (*Repsol-YPF, Argentina)* and Rocky Roden (*Repsol-YPF, U.S.A.)* for their help, and Repsol YPF for their permission to publish this work.

Determinação do Limite Crustal na Margem Centro-Leste Brasileira
Integração de um Novo Método com Modelagens Crustais e Mapeamento Sísmico

Joao Bosco Monteiro Rodarte, PETROBRAS S/A, Brasil, jrodarte@petrobras.com.br

Resumo

Nesse trabalho apresenta-se o *método Anaccor*, um novo método de análise e determinação do limite entre as crostas continental e oceânica, cuja técnica se baseia na utilização combinada da gravimetria e da magnetometria. Esse método foi desenvolvido durante a realização de uma análise regional da Margem Centro-Leste Brasileira, quando se fez uma interpretação integrada de dados geológicos e geofísicos, definindo-se o arcabouço estrutural do embasamento, a compartimentação das bacias, e a geometria da faixa rifte.

Como as principais rochas geradoras são da seqüência rifte, o limite exploratório das bacias está diretamente relacionado à largura da faixa rifte, estendendo-se para leste até o limite entre as crostas continental e oceânica. A determinação desse limite tem sido assunto polêmico, estando ainda sujeito a diferentes interpretações, devido principalmente à falta de uma metodologia mais objetiva. Para minimizar esse problema procurou-se obter o limite crustal através de três métodos.

Os dois primeiros métodos já são usualmente consagrados, sendo que no primeiro define-se o limite crustal através de modelagens crustais, ajustando-se as anomalias gravimétricas e magnéticas observadas, às anomalias calculadas pelo *método de Talwani*; no segundo utiliza-se o *método sísmico*, reconhecendo-se a crosta oceânica como um conjunto de reflexões com padrão incoerente, descontínuo, e de altas amplitudes.

Apesar do caráter empírico, o *método Anaccor* tem a vantagem de ser menos ambíguo e subjetivo do que os dois métodos citados anteriormente, já que o domínio de crosta oceânica pode ser detectado através do reconhecimento de um padrão de correlação negativa entre os perfis gravimétrico e magnético.

Introdução

A Margem Centro-Leste Brasileira compreende as bacias de Campos, Espírito Santo, Cumuruxatiba, Jequitinhonha, Almada e Camamu (Fig. 1).

O avanço da fronteira exploratória para o domínio de águas profundas, torna indispensável os estudos regionais de análise de bacias, com enfoque no arcabouço estrutural do embasamento, e na caracterização de possíveis sistemas petrolíferos. A determinação do limite entre as crostas continental e oceânica tem importância na definição do limite exploratório das bacias, marcando o limite leste da faixa rifte e consequentemente a área de ocorrência das principais rochas geradoras, geralmente associadas à seqüência rifte.

Metodologia

A interpretação sísmica regional da Margem Centro-Leste Brasileira foi precedida de uma análise comparativa entre as feições estruturais observadas nos mapas residuais gravimétricos e nas linhas sísmicas.

Inicialmente escolheu-se um conjunto de linhas-guias regionais representativas de cada bacia, cuja interpretação foi inicialmente utilizada nas modelagens crustais, e extrapolada posteriormente para a malha sísmica completa. De modo geral ficou evidente a boa correlação entre as estruturas imageadas pela sísmica com os *trends* estruturais dos mapas residuais gravimétricos.

O embasamento em tempo das linhas-guias foi então convertido para profundidade, obtendo-se os modelos geológicos iniciais para as modelagens gravimétricas e magnéticas. Nessas modelagens, o cálculo da resposta gravimétrica regional do manto, foi ajustado à componente regional das anomalias observadas, definindo-se a profundidade e a forma da interface crosta/manto em cada bacia. Na maioria dos perfis, as anomalias residuais calculadas se ajustaram às anomalias residuais observadas, provavelmente devido ao ajuste prévio entre os arcabouços estruturais obtidos a partir da gravimetria e da sísmica. Quando necessário, devido a alguma dificuldade de imageamento do embasamento e da seção rifte, a profundidade do embasamento foi modificada no modelo geológico de entrada, procurando-se o melhor ajuste entre as anomalias residuais observadas e calculadas. De posse dos modelos crustais ajustados em todas as linhas-guias, o modelo do embasamento em profundidade de cada uma dessas linhas foi então reconvertido em tempo e amarrado à malha sísmica restante, completando-se a interpretação regional.

O limite crustal determinado inicialmente através de modelagens crustais, foi corroborado posteriormente pelo mapeamento sísmico regional, quando observou-se que os dados gravimétricos e magnéticos apresentavam padrões de resposta visivelmente defasados no domínio de crosta oceânica. A partir dessas observações, desenvolveu-se o *método Anaccor*, que determina a posição do limite crustal a partir de uma análise da correlação dos dados gravimétrico e magnético ao longo de um mesmo perfil.

Nesse método, o ponto de partida são os mapas de anomalias free-air e do campo magnético total, cujos dados passam por um processamento prévio, incluindo-se o cálculo de derivadas horizontais e normalização. A partir desses dados obtém-se os perfis gravimétrico e magnético, que são então superpostos em um mesmo gráfico, de modo a facilitar a análise comparativa.

Análise dos resultados

A geometria básica da compartimentação de blocos e sub-bacias da Margem Centro-Leste Brasileira é caracterizada por um padrão sigmoidal de rombo-grabens escalonados, definido pelo entrecruzamento de falhas longitudinais de rejeito normal, e falhas transversais com características de falhas de transferência. A compartimentação das bacias foi definida de acordo com a profundidade do embasamento, caracterizando-se quatro domínios crustais, três em crosta continental, e um em crosta oceânica.

Os dois primeiros domínios tem menor grau de estiramento crustal e incluem a zona emersa e a zona de plataforma submersa em águas rasas, onde o embasamento é relativamente mais raso.

O terceiro domínio, em águas profundas, inicia-se na zona de talude e pode ser associado a um maior grau de estiramento crustal e a maiores profundidades do embasamento.

Próximo ao limite leste da faixa de crosta continental estirada, observa-se uma diminuição gradativa da profundidade do embasamento e da espessura do rifte, atingindo-se bruscamente um assoalho oceânico sub-horizontal de constituição basáltica, que marca o início do quarto e último compartimento crustal, o domínio de crosta oceânica.

A análise de quatro perfis representativos, ilustram a integração dos três métodos na determinação do limite crustal, (Fig. 2).

Através do *método Anaccor*, observa-se que no domínio de crosta continental os perfis gravimétrico e magnético ficam em fase e quase paralelos (correlação positiva), enquanto que no domínio de crosta oceânica esse padrão é visivelmente defasado, ou seja, quando o perfil gravimétrico é positivo, o perfil magnético é negativo e vice-versa (correlação negativa), (Figs.3a a 6a).

Nas modelagens crustais, o limite crustal está associado a um contraste de susceptibilidade magnética entre a crosta continental siálica e a crosta oceânica de constituição máfica (basalto e gabros), (Figs.3b a 6b).

Em linhas sísmicas, o limite crustal coincide com o ponto em que o caráter sísmico contínuo, coerente e de baixo contraste de impedância do topo do rifte passa para um padrão sísmico de reflexões descontínuas, incoerentes, e de alto contraste de impedância, que geralmente aparecem associadas a difrações residuais não corrigidas pelo processo de migração sísmica, (Figs.3c a 6c).

Conclusões

Enquanto que o *método de Talwani* associado ao *método sísmico* definem uma faixa de até 60 km para a localização do limite crustal, a integração desses dois métodos com o *método Anaccor* permitiu uma definição mais precisa do limite crustal, marcando o final da faixa rifte e o início do domínio de crosta oceânica.

A delimitação da faixa rifte, bem como a definição da geometria do rifte da Margem Centro-Leste Brasileira, pode ser extrapolada para o contexto megarregional da tectônica de placas, reconhecendo-se uma correspondência e um encaixe entre os limites crustais das placas SulAmericana e Africana, permitindo a reconstrução paleogeográfica do Atlântico Sul ao final da fase rifte (Eo-Aptiano/ Neo-Aptiano).

Além disso, a partir de trabalhos e mapas regionais da costa oeste africana (ex., Karner et al., 1997; Karner and Driscoll, 1999), foi possível reconhecer a correspondência entre as bacias conjugadas das margens centro-leste brasileira e centro-oeste africana.

Referências

Karner, G.D., Driscoll, N.W., McGinnis, J.P., Brumbaugh, W.D., and Cameron, N.R. 1997, Tectonic significance of syn-rift sediment packages across the Gabon - Cabinda continental margin. Marine and Petroleum Geology, vol. 14, n. 7/8, p. 971 - 1000.

Karner, G.D. and Driscoll, N.W. 1999, Tectonic and stratigraphic development of the West African and eastern Brazilian margins: insights from quantitative basin modelling. In: Cameron, N.R., Bate, R.H. and Clure, V.S. (eds.), The oil and gas habitats of the South Atlantic. Geological Society, London, Special Publications, 153, 11-40.

Rodarte, J.B..M., Pereira, M..J., Mohriak, W.U., Lyrio, J.C.S.O., Caddah, F., Telles, A.S.,1999,A geometria do rifte na Margem Centro-Leste Brasileira e suas possíveis relações com as acumulações de hidrocarbonetos.PETROBRAS-E&P-BA-GEXP-GEINT- Salvador, 1999 - Relatório 110C-11597, p. 1- 33.

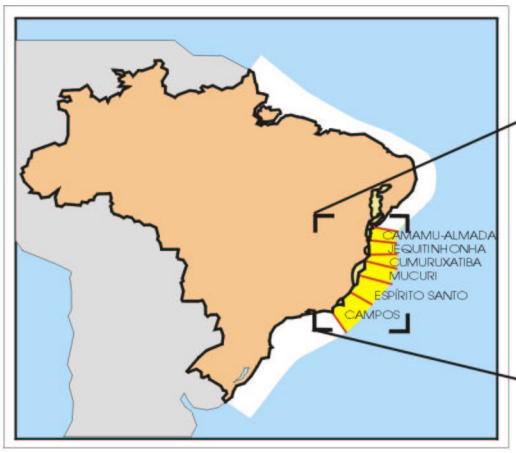

Fig. 1: Mapa de localização das bacias costeiras da Margem Centro-Leste Brasileira

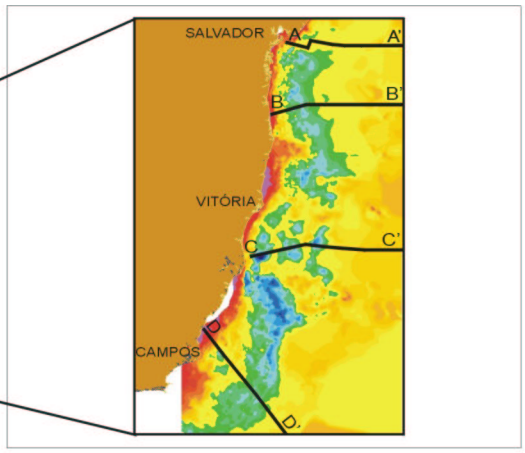

Fig. 2: Mapa estrutural sísmico do embasamento e localização dos perfis analisados

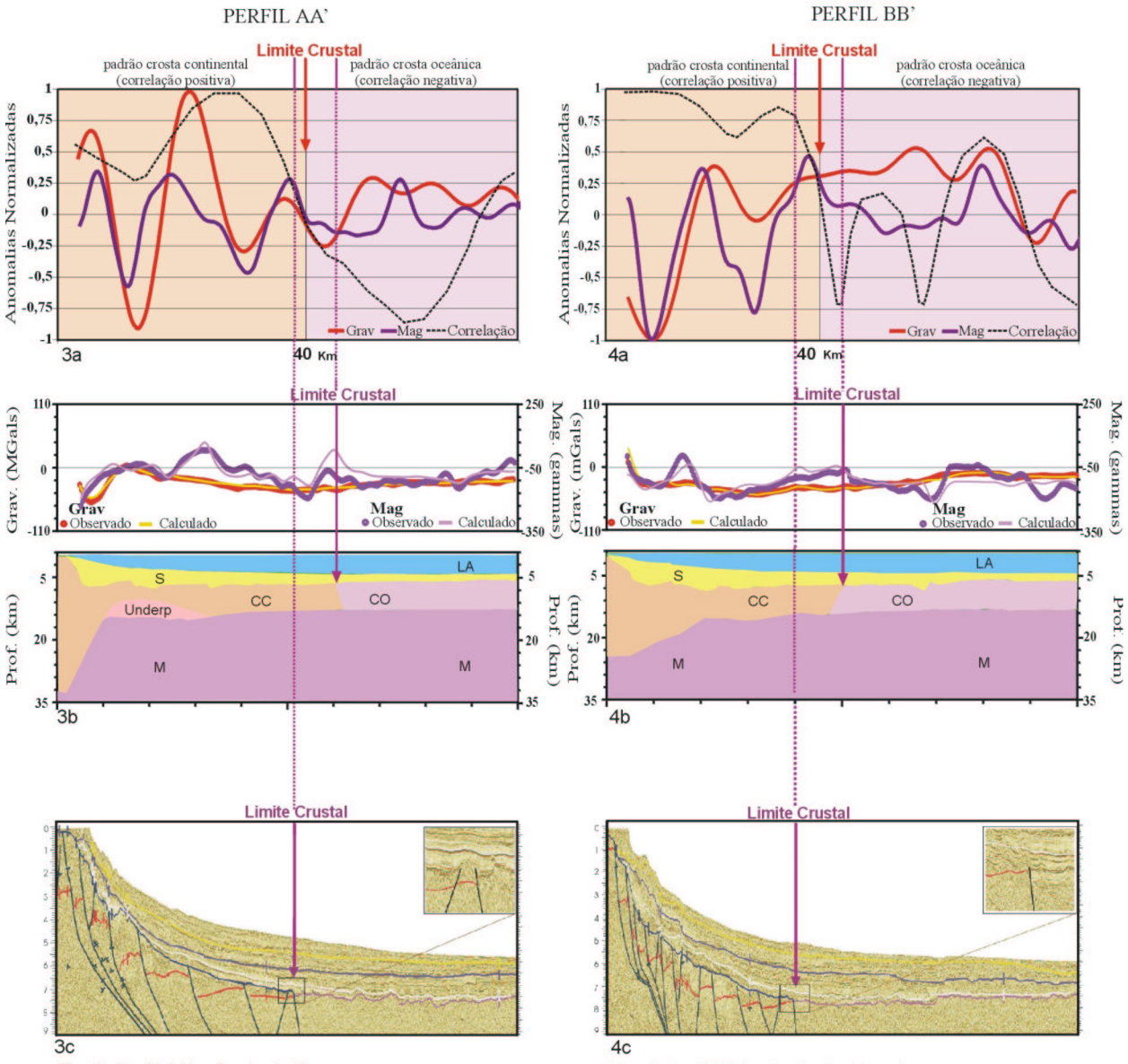

Fig. 3: Perfil AA' - Bacia de Camamu

Fig. 4: Perfil BB' - Bacia de Almada

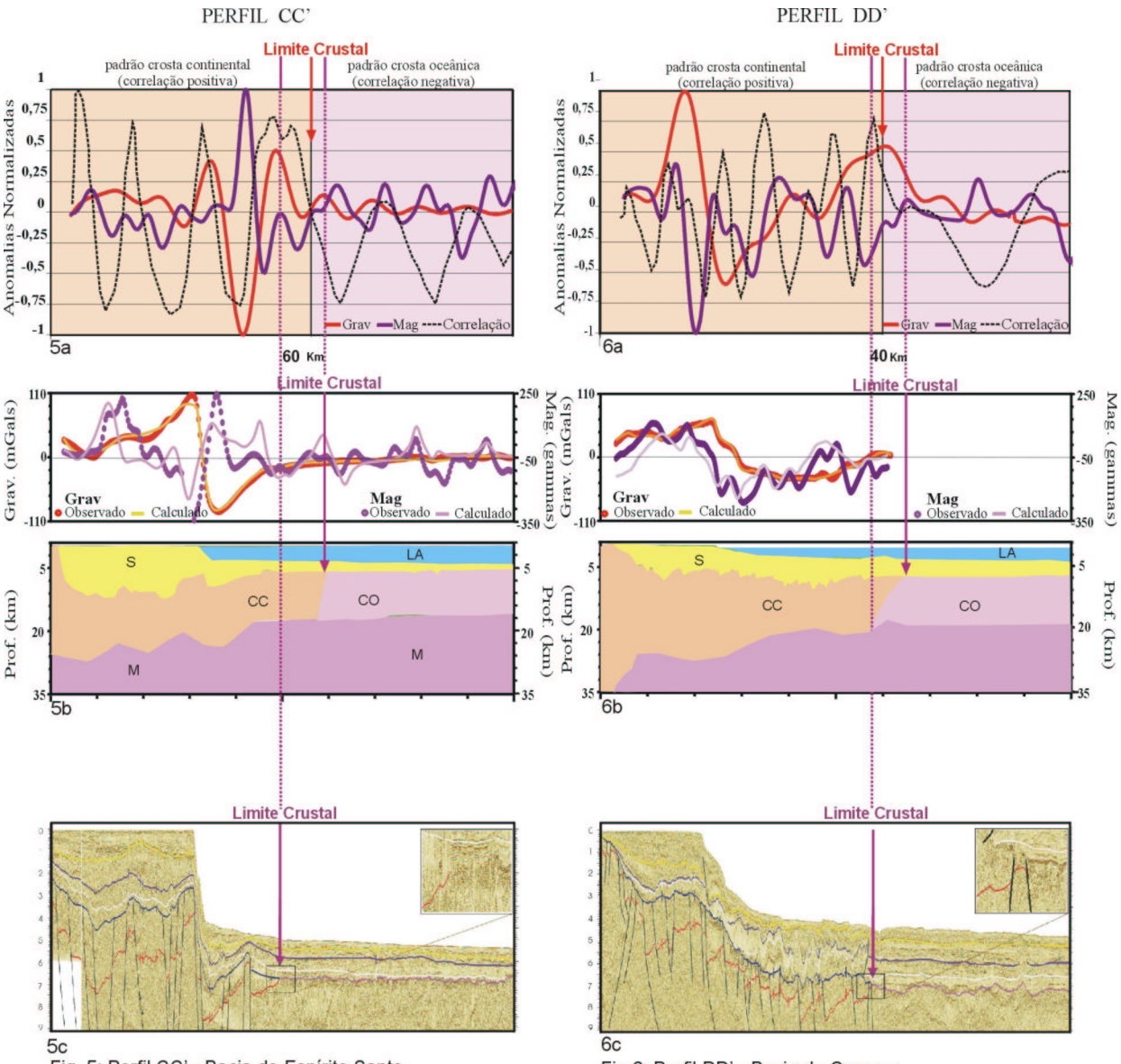

Fig. 5: Perfil CC' - Bacia do Espírito Santo

Fig.6: Perfil DD' - Bacia de Campos

EL "HOYO DE OROCUAL" … UNA CURIOSIDAD GEOLOGICA, IMPACTO DE METEORITO o ESTRUCTURA DE COLAPSO.

Gilberto Parra, PDVSA, parragi@pdvsa.com
Pedro Villarroel, PDVSA, villarroelp@pdvsa.com
Juan Guevara, PDVSA, guevarajq@pdvsa.com
Gustavo Carvajal, PDVSA, carvajalge@pdvsa.com

RESUMEN:

El "hoyo de Orocual" es una curiosa estructura geológica, la cual ha sido objeto de numerosas interpretaciones a lo largo de la historia del campo, se encuentra ubicado al norte del edo. Monagas, al este de Venezuela, figura N° 1.
En este trabajo presentaremos todas las teorías que han tratado de explicar el origen de "Hoyo", la mayoría se refiere a una estructura de colapso asociado a los corrimientos del frente de deformación y al diapirismo de lodo característico del norte de monagas, figura N° 2,sin embargo existe un buen número de geólogos que piensan que puede tratarse del impacto de un meteorito, y considerando que existen unos quince campos petroleros asociados a impactos de meteoritos la idea no es ilógica. PDVSA Exploración y Producción, por medio de la Unidad de Explotación Norte asumió a finales de 1997, la gerencia del viejo campo Orocual somero, el mismo está localizado en el norte del estado Monagas, al sur del cinturón plegado conocido como la Serranía del Interior, con la finalidad de buscar nuevas oportunidades que permitan incrementar la producción, se conformó un equipo multidisciplinario, combinando la geociencia, el conocimiento de la ingeniería de reservorio y de producción, utilizando nuevas tecnologías de perforación y rehabilitación, basado en la revisión de la poca información dinámica y estática disponible.
Como parte de estas actividades, y para hacer a un modelo sísmico estructural del área, se llevó a cabo la interpretación sísmica 3D, con 200 Km^2 de información sísmica del proyecto OROCUAL-93, diseñado para objetivos profundos. El levantamiento de OROCUAL-93 cubre el 100% del área de estudio y los pozos perforados se ubican dentro de sus límites. Para la interpretación se utilizó una versión reprocesada a fase cero y amplitud preservada por considerarse que es de mejor calidad que la versión original.
El levantamiento OROCUAL-93, conformado por 1300 líneas orientadas NW-SE y 700 trazas orientadas SW-NE, cubre un área de 200 Km^2 interpretados totalmente en cuanto a pozos se refiere, se utilizaron los datos de 110 pozos. En el área existen 14 pozos con datos de velocidad que permitieron calibrar la sísmica con los pozos, se realizaron los sismogramas sintéticos de estos 14 pozos.

DESCRIPCIÓN:

Se interpretaron cinco marcadores sísmicos regionales para un mejor control de la estructura, en la cual cabe destacar la presencia de una depresión de casi 3 Kms de diámetro y 4000 pies (1200 metros) de calidad, dentro de esta estructura la acumulación está en compartimientos estructurales, cuya prospectividad radica en que dentro de la misma se acumulan hidrocarburos livianos, medianos, fuera de este "hoyo" la acumulación es de crudo pesado, al lado de esta estructura se encuentra un anticlinal el cual está genéticamente relacionado con el "hoyo", ver figura N° 3.
Las fallas se comenzaron a interpretar en forma paralela a la sedimentación al este de la zona de estudio en virtud de que la mayoría de las fallas son de tipo normal y buzan al sur con dirección SW-NE, al oeste del área de estudio la dirección del sistema de fallas se orienta NW-SE, son normales y buzan al oeste, razón por la cual las líneas se interpretaron perpendicular a la dirección de la sedimentación. En la zona de la estructura de colapso se interpretó tanto en las "inlines" como en las "crosslines", además de líneas arbitrarias para la definición de las fallas, en su mayoría normales. La generación de secciones horizontales constituyeron una herramienta fundamental en la comprensión del sistema de fallas, pero muy en particular en la zona del colapso. La interpretación y animación sísmica con el módulo de Seiscube fue muy útil familiarizarse con el sistema de las fallas. Casi simultáneamente con la interpretación se triangularon e interpolaron los segmentos de las fallas de interés, para la posterior generación de los polígonos de fallas y validación de los planos con respecto a pozos fallados.
En el área de Orocual existen 14 pozos profundos y dos someros con datos de velocidad. Estos datos fueron cargados en la aplicación SEISWORK™ de la compañía LANDMARK GRAPHICS Co. en la elaboración de sismogramas sintéticos y el modelo de velocidad, se calcularon los pares tiempo-profundidad, valores de velocidad promedio y velocidad interválica calculadas a partir de los mismos así como sus respectivos gráficos.
Para realizar la calibración pozo-sísmica se generaron 14 sismogramas sintéticos. La calibración sísmica-pozo es en general de buena calidad. Se debe

mencionar que en ciertos casos se aplicó un desplazamiento "shift" a las curvas de velocidad a manera de asegurar una correlación adecuada con la sísmica.

RESULTADOS:

La calidad de los datos para la Formación Las Piedras puede ser subdividida en tres áreas principales:

En el Área del diapiro, la calidad de la sísmica es de regular a buena los reflectores son relativamente fuertes y muestran buena continuidad lateral, facilitando la cartografía y delineado del diapiro. El diapirismo fracturó completamente los estratos superiores, y ocasionó un extenso fallamiento en su tope, aunque lateralmente las reflexiones muestran continuidad y son cartografiables.

El Área Norte, presenta una calidad de datos de regular resolución lateral en la zona productora.

En el Área de la Estructura de Colapso, por la propia naturaleza la masa homogénea prácticamente no ofrece contraste de impedancia acústica, en consecuencia no hay reflexiones, en gran parte de la estructura de colapso no es posible seguir reflector alguno, ya que la señal sísmica está altamente perturbada, ningún reprocesamiento podría mejorar esta situación. El área del hoyo va disminuyendo con la profundidad, mejorando ligeramente la resolución lateral. Se interpretó la estructura la cual corresponde a un monoclinal con buzamiento promedio 10° al sureste, alterado por un hoyo y un anticlinal orientados en sentido SSW-NNE, figura N° 4.

En la línea de trabajo que hemos seguido, se analizaron varios modelos estructurales que podrían explicar la formación de la estructura de colapso y el anticlinal como consecuencia del diapirismo de lodo, el modelo propuesto – sin pretender tener la última palabra - consiste en un sistema de fallas tipo "cola de caballo" *sensu lato*, estos sistemas fueron muy bien descritos por Chinnery, 1966, ver figura N° 5.

Los segmentos de fallas en colores ocre, amarillo, fucsia, naranja, verde, amarillo y marrón claro, corresponden al sistema principal de transcurrencia, la respuesta sísmica de forma elipsoidal indica la presencia del anticlinal producto del diapiro de lodo. Las fallas representadas en color amarillo se insinúan en las secciones horizontales, en las secciones verticales es prácticamente imposible observarlas, este patrón es característico de las fallas asociadas la falla transcurrente principal, las orientadas en sentido NO-SE, corresponderían al patrón tipo riedel (R shears), las fallas orientadas en sentido NE-SO podrían corresponder a los patrones R' shear y/o P shear.

En la zona oeste del área de estudio se aprecia un patrón de fallas con orientación preferencial norte-sur, las mismas son de carácter normal, con evidencia de rotación entre los bloques a ambos lados de las fallas, las mismas presentan una separación vertical estimada de 50 a 80 pies. Este rasgo estructural tiene similitud con el modelo de Chinnery, 1966, correspondiente al Tipo B.

La estructura de colapso de Orocual corresponde a una depresión de forma elipsoidal, su eje más largo de 1500 m aprox., en sentido SO-NE, es decir, con la misma dirección del diapiro, su eje corto se encuentra en dirección casi perpendicular al eje principal., El diámetro promedio es de 3 kms, con un desnivel de 4200 pies(1280 m). La parte más profunda del hoyo está ubicada al norte, el pozo ORS-21 penetró el tope de la Fm. Carapita @ 7631'.

Su peculiar fallamiento puede subdividirse en dos patrones, un patrón de fallas concéntricas subverticales de carácter normal, con saltos verticales que van desde 100 pies y hacia el norte del hoyo pueden superar los 2000 pies. El otro sistema de fallas es pseudoradial, también fallas subverticales, normales, generandose una gran cantidad de compartimientos estructurales, donde prácticamente cada pozo está en un bloque. De este segundo patrón de fallas destaca la falla color morado la cual refleja un movimiento de transcurrencia dextral. El rango de buzamiento de las capas se encuentra en el orden de los 14°-54°, hacia el borde del hoyo se presentan los buzamientos más elevados, y sísmicamente todavía se observa buena señal. La cartografía dentro del hoyo se apalancó en el número de pozos concentrados en el hoyo, datos de buzamientos, datos de producción, secciones sísmicas horizontales y verticales.

El trabajo siguiente será la restauración y balanceo de secciones a fin de descartar inconsistencias en la interpretación.

Sin embargo existen rasgos morfológicos del "hoyo" que se insinúan como un cráter producto del impacto de meteorito teoría que aún no ha sido lo suficientemente defendida.(Figura N° 6).

CATEGORÍA TÉCNICA:

INTERPRETACIÓN SÍSMICA.

EL "HOYO DE OROCUAL"

FIGURA N° 1 Mapa de ubicación.

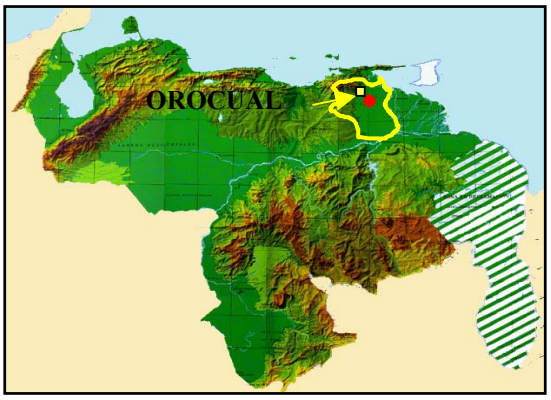

FIGURA N° 2 Corte esquemático del campo.

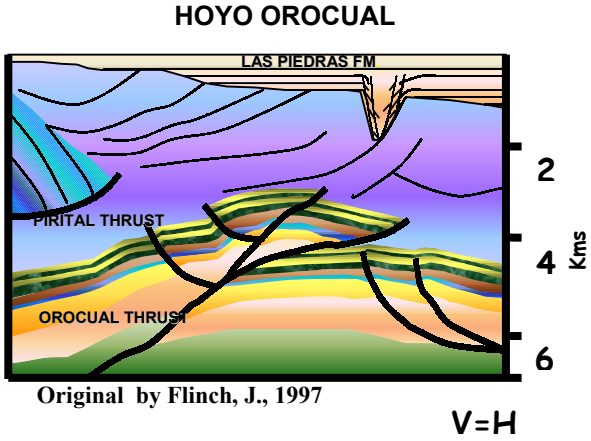

FIGURA N° 3 Time slice mostrando el hoyo y el diapiro.

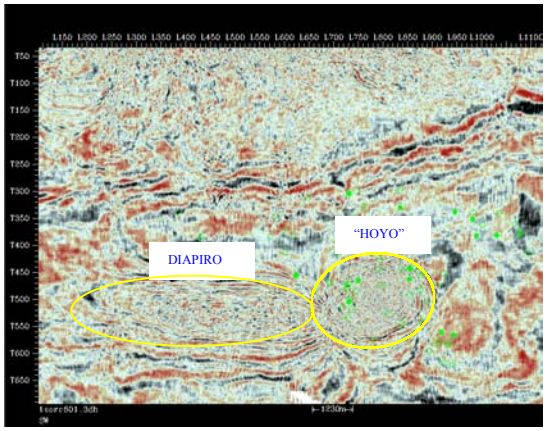

FIGURA N°4 Modelo estructural interpretado.

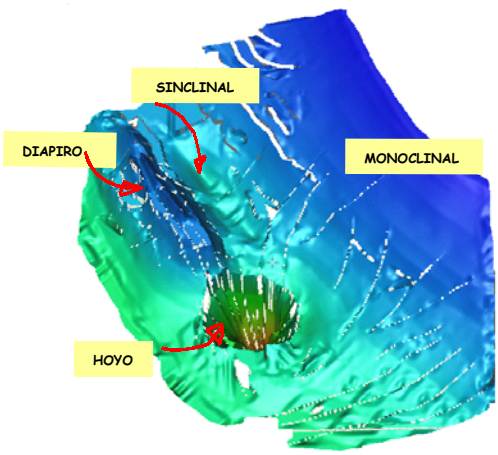

FIGURA N° 5 *Modelo básico de Chinnery, 1966.*

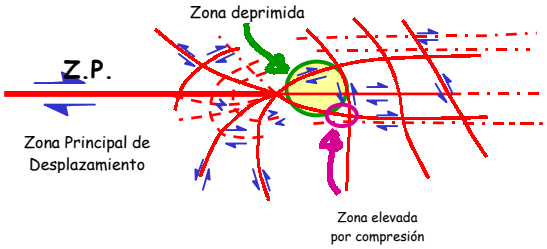

EL "HOYO DE OROCUAL"

FIGURA N° 6 Teoría del impacto y su posible Trayectoria

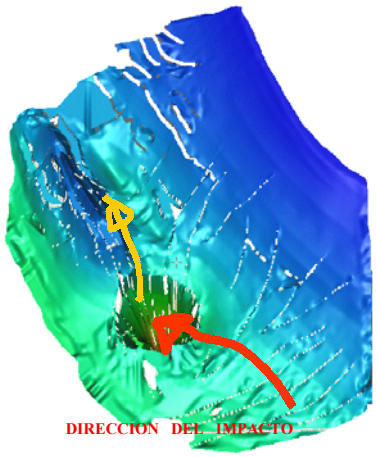

Growth Folding in Gravitational Fold-and-Thrust Belts in the Deep Waters of the Equatorial Atlantic, Northeastern Brazil

Pedro Victor Zalán, PETROBRAS S/A, Brazil

Introduction

As the continental margins build outward into deep and ultra-deep waters via continuous denudation of the adjoining shields and sedimentation of the debris forming the continental shelves and slopes, the rifted/thinned edge of the continental plates cool exponentially as they move away from the heat source that created the rupture and breaking of the former larger continental plate. These create a very unstable situation since large volumes of sediments pile up at the margin of the continental shelves, in the upper slope, at the same time the whole area is gradually tilting oceanward due to thermal flexural bending. Gravity failure occurs and allochtonous masses of sediments slide down the slope, over a plastic lithology that acts as a lubricant and detaches the traveling rocks above from the autochtonous rocks below. When the frontal parts of the allochton diminish their velocity due either to a decrease in the gradient of such detachment zone or to a physical barrier (commonly a volcanic edifice) the incoming allochtons collide and strong contraction/compression occurs.

The failure occurs when vertical stresses due to overburden are weakened in relation to sub-horizontal stresses due to several possibilities, including overpressure in shales (due to petroleum generation or any other classical overpressure mechanism) or ductile flow in salt. Shear stresses develop parallel to the slightly dipping bedding and overcome the vertical stresses

These deformed masses of allochtonous rocks are nowadays referred to as ***linked extensional-compressional systems*** and have been found in the deep/ultra-deep water regions of most continental margins around the world. It is easily understood, and very well displayed in modern seismic sections, that these systems are composed of three major tectonic domains, each one presenting different and peculiar deformation (Figure 1).

The ***extensional domain*** comprises highly strained subsided terrains at the upper continental slope, dominated by arcuated listric normal faults that sole out at the detachment level. Major listric faults present significant associated rollover anticlines and growth depositional wedges that thicken from the crest of the anticline towards the listric fault. Subsidiary listric normal faults, antithetic to the major downdip listric faults, are also abundant, as well as crestal fracturing/faulting in the rollover anticlines.

The ***translational domain*** is a predominantly non-deformed region, that passively traveled over the detachment zone. Weak arching may affect the rocks present in this area.

The ***compressional domain*** may present spectacular deformation, with all kinds of reverse and thrust faults and fault-related folding (detachment, fault-propagation and fault-bend folding). When detached on shales, the structural styles and dimensions may resemble those found in truly orogenic belts (Zalán 1998). When salt is the lubricant, deformation is more complex and salt canopies develop. The specific name ***gravitational fold-and-thrust belts (GFTB's)*** have been applied to such entities. Zalán (1999) studied some brazilian GFTB's in detail and devised a tripartite structural model that predicts an orderly succession, from the internides to the foreland, of detachment folding, followed by high-angle reverse faults and associated fault-propagation folds, ending in low angle, ramp-flat thrusts with associated fault-bend folding. Important oil discoveries have been achieved in these compressional provinces in deep waters off Nigeria Angola, GOM and Brazil.

The dimensions of these three domains may vary greatly. Usually the extensional and compressional domains are the widest but it is very difficult to exactly balance the amount of extension updip with the amount of contraction downdip, because of the details of the severe deformation that is usually non-resolvable by the volumes of seismic data available. Since they cover huge areas, in the order of several thousand square kilometers, it is difficult to have them all covered by 3D seismic, and it is not unusual that extension and compression be divided into two or three belts of deformation.

GFTB's with Growth Folding

When the process of gravity sliding/contraction is long-lasting (10-40 m.y.) and takes place in areas with low rates of sedimentation the peculiar mechanism of growth folding comes into scene. Since GFTB's develop in exclusively submarine environments, they are never subaerially exposed, sedimentation takes place concomitantly with the compressional deformation leading to the deposition of syntectonic growth strata that thin up onto the upper parts of the foldbelt, in the same way the growth wedges develop in the downthrown sides of the normal faults in the extensional domains.

Medwedeff (1989) unraveled complex growth stratigraphic relationships between coeval sediments deposited in the forelimb and back-limb of a single fault-bend fold in California. Numerous wells and seismic data allowed the author to deduce that syntectonic sedimentary strata onlap a time-transgressive unconformity on the forelimb but have uniform dip and constant thickness, and are folded below the unconformity on the back-limb (Figure 2).

Same age sediments are deposited over the positive topographic expression of the fold (forelimb) in onlap pattern, as well as conformably over the horizontal strata that is traveling towards the deformation locus (back-limb). These horizontal strata have constant thickness and are rolled through an active axial surface forming the back-limb of the fold that will continuously grow towards the internal part of the deformation, while the forelimb will be passively transported in the other direction towards the foreland. A time-transgressive unconformity continuously develops in the same direction as the fold grows, toward the internides, and erodes/covers the sediments that are folded and uplifted in the back-limb.

The same mechanism seems to be applicable to GFTB's in the Brazilian equatorial atlantic margin, such as the Pará-Maranhão, Barreirinhas and Touros GFTB's. Figure 3 shows an interpreted depth seismic section from the Pará-Maranhão Basin, where three reflectors can be correlated across four time-transgressive unconformities (dark yellow). These reflectors (dark green, purple and blue) are interpreted to encompass the growth strata associated to this GFTB.

The geometry of the deformation in this GFTB suggests that the folding and uplift of the thrust strata was a long-lived process. Since there is a major long-lasting time-transgressive unconformity (as well as three minor ones) that separates the non-deformed strata above from the deformed strata below it is plausible to deduce that the rates of sedimentation were low, the uplifted/folded/thrust strata was left exposed at the sea bottom and submarine erosion (currents) could take place.

The same pattern of a series of younging- and stepping-upward time-transgressive unconformities separating non-deformed onlapping strata above from thrust and folded strata below can be seen in several other GFTB's in Brazil (Barreirinhas and Touros) and elsewhere in the world (for instance, in the Krishna-Godavari Basin, in India) and are here interpreted as being diagnostic of gravity sliding/contraction accompanied by growth folding in areas dominated by low rates of deformation and sedimentation.

GFTB's without Growth Folding

Some GFTB's do not display the complicated pattern of time-transgressive unconformities as described above. They involve thick packages of sediments that are folded and thrust harmonically. Syntectonic sedimentation seems to follow a simpler and more easily understood pattern of being confined to intervening synclines between anticlines. In this case, the syncline packages typically thicken downward towards the depocenter and thin upward towards the anticlines. Such is the case in the Foz do Amazonas (Figure 4), Cone do Rio Grande and Niger delta GFTB's, where all allochtonous sediments are harmonically folded and thrust up into the sea bottom. They are situated in front of young deltas (Miocene) where huge piles of sediments accumulated very quickly in a very short time, while gravity sliding was taking place, also during the same short time.

The pattern of harmonically folded and thrust sediments, with thick syntectonic packages in the synclines and thinner correlative packages on the anticlines, and more importantly, the absence of time-transgressive unconformities, are here interpreted as being diagnostic of gravity sliding/contraction in areas dominated by high rates of deformation and sedimentation.

The major implications for such differences in the depositional/structural styles of the growth strata are in the location of the turbidite beds and the related hydrocarbon traps.

References

Medwedeff, D.A., 1989, Growth fault-bend folding at southeast Lost Hills, San Joaquin Valley, California: AAPG Bulletin, v.73, p. 54-67.

Zalán, P. V., 1998, Gravity-driven compressional structural closures in Brazilian deep-waters: a new frontier play: AAPG Annual Meeting Extended Abstracts vol. 2, Salt Lake City, Utah, p. A723.

Zalán, P.V., 1999, Seismic expression and internal order of gravitational fold-and-thrust belts in Brazilian Deep Waters (expanded abstract): Sixth International Congress of the Brazilian Geophysical Society, CD-ROM with Extended abstracts, Rio de Janeiro, August, 4 p.

Zalán, P.V., 2001, Growth Folding in Gravitational Fold-and-Thrust Belts in the Deep Waters of the Equatorial Atlantic, Northeastern Brazil: AAPG Annual Convention Official Program Book and CD-ROM, Denver, June, p. A223.

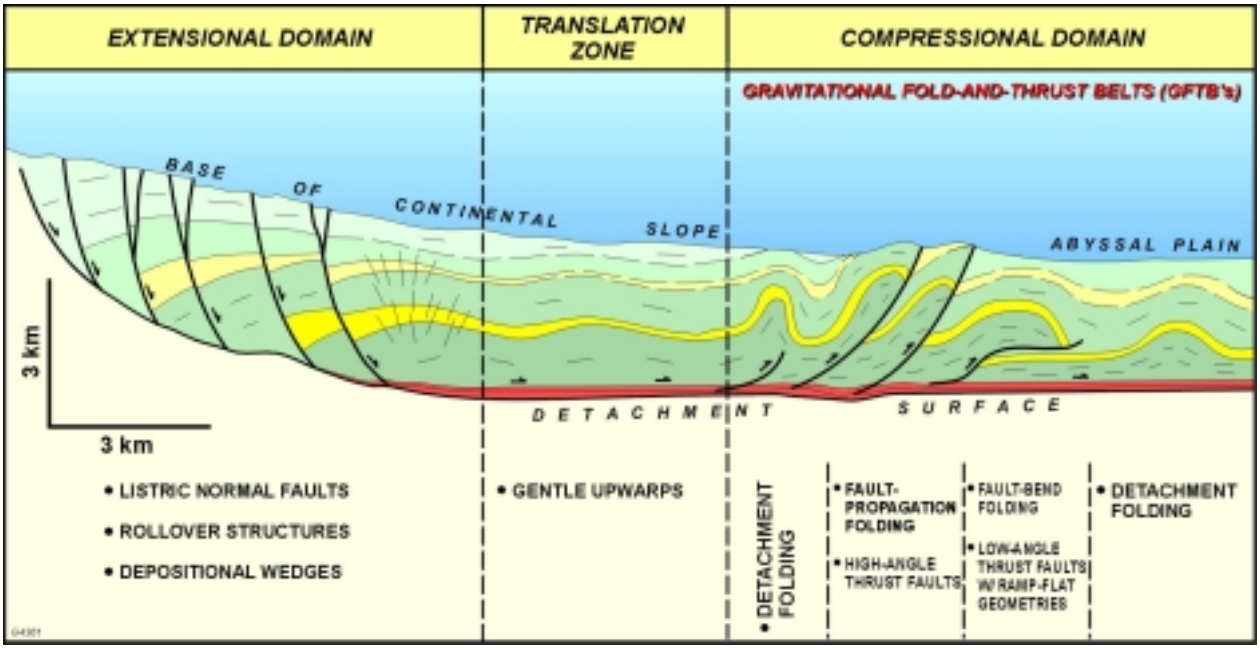

Figure 1 – Linked extensional-compressional systems (linkage via detachment surface) consist of three major tectonic domains: extensional, translational and compressional, each with their own specific structural style. The compressional domain is usually called ***gravitational fold-and-thrust belts (GFTB's)*** and the style here illustrated depicts the situation of a non-mobile shale-cored detachment zone. When the GFTB is cored in mobile plastic lithologies such as salt, or even shale, more complex deformation is created (diapirs, salt canopies, disharmonic folding)

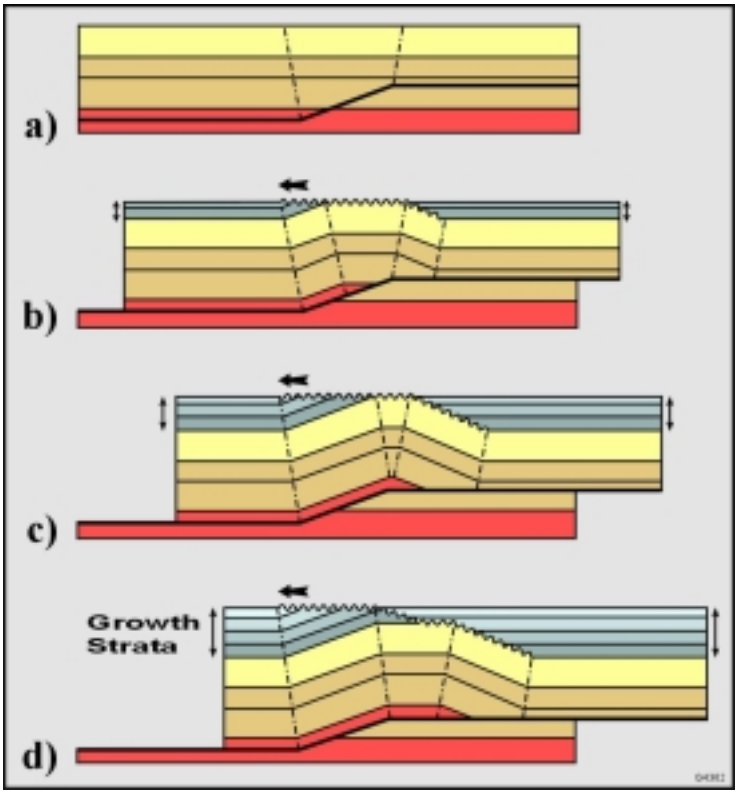

Figure 2 – Growth folding mechanism devised by Medwedeff (1989) for a fault-bend fold in California.

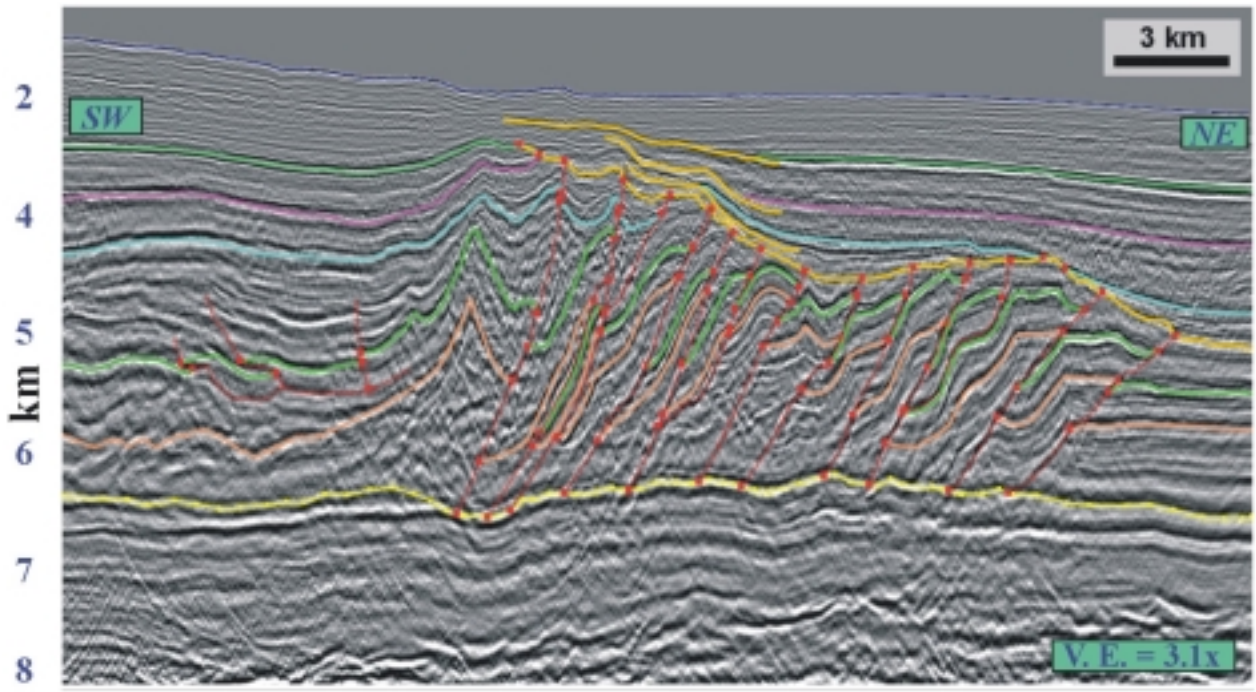

Figure 3 – Depth migrated seismic section showing the GFTB from the Pará-Maranhão Basin, interpreted according to the concepts of growth folding described above. Dark yellow reflectors indicate time-transgressive unconformities in a younging- and stepping-upward pattern. Blue, purple and dark green reflectors are interpreted both above and below such unconformities and encompass the growth strata of the GFTB. Light green and orange reflectors are pre-tectonic strata and light yellow represents the detachment zone.

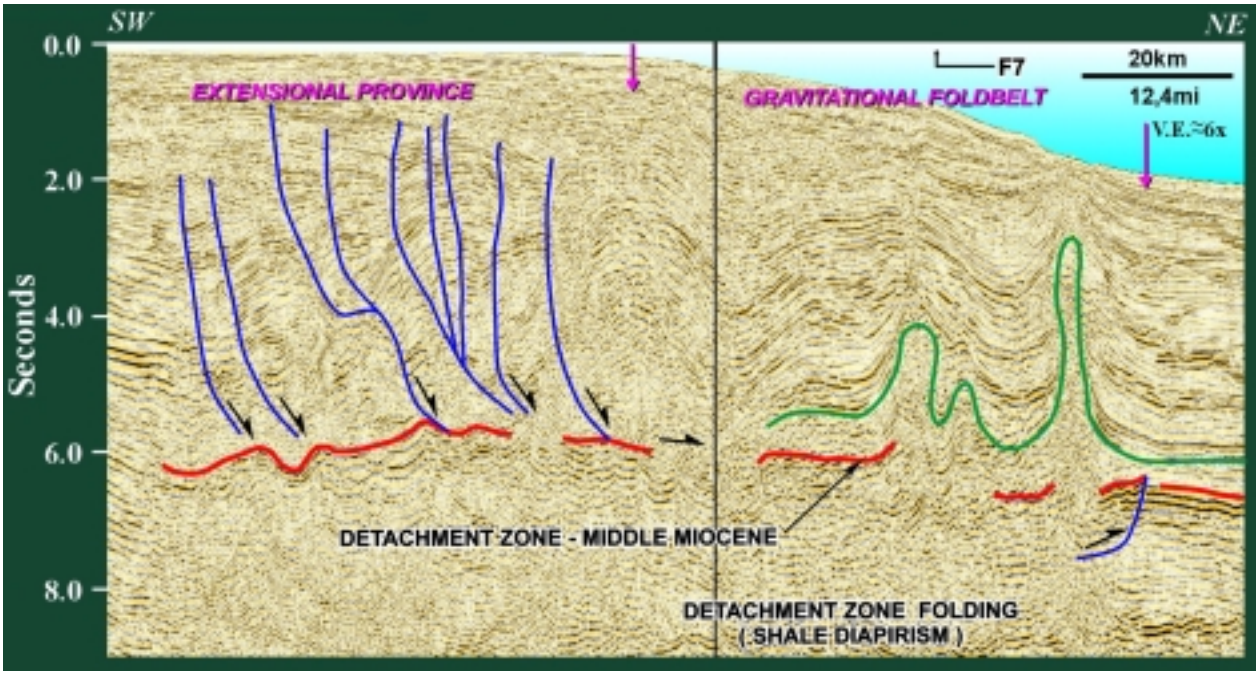

Figure 4 – Time seismic section showing the GFTB from the Foz do Amazonas Basin. Diapiric mobile shale nucleates the detachment folds in the compressional domain. Notice the absence of unconformities in the upper parts of the compressional domain, that seems to affect up almost to the sea bottom. The main reason for such difference in structural styles is attributed to much higher rates of sedimentation and deformation related to the Amazon delta, in contrast with the Pará-Maranhão GFTB which lacks contribution from any significant delta.

Reservatório Turbidítico da Bacia de Campos – Um estudo de detalhe

Marcos Sebastiao dos Santos, PETROBRAS S/A, Brasil

Abstract

This paper is about a madure field in Campos Basin – Brazil. It reports the seismic support given to an integrated study of reservoir which hole is to reach a good simulation.
The seismic interpretation was made with the support of amplitude seismic and acoustic impedance data. Detailed geological sections was constructed with seismic support in the sense of helping the reservoir understanding.
The turbidites reservoir was divided in five sequences. The seismic just couldn't help the separation of two of them.

Introdução

O campo estudado localiza-se na Bacia de Campos. Hoje, encontra-se em fase avançada de desenvolvimento, com mais de 50 poços perfurados.

O presente trabalho descreve a interpretação sísmica de detalhe efetuada no campo; parte de um estudo integrado, cujo objetivo é fornecer um modelo de fluxo mais realista, e em malha menor do que a usada no passado. Na fase de produção em que se encontra o campo, com todos os poços perfurados, alguns deles já abandonados ou transformados em injetor, um estudo como esse busca otimizar ao máximo os percentuais de recuperação.

Os reservatórios correspondem a turbiditos de idade albiana/cenomaniana. A deposição é controlada pelos eventos tectônicos correlacionados à movimentação halocinética, sendo a porção inferior do pacote bastante confinada à calhas correlatas a esses eventos. De mesma geração, observam-se falhamentos que compartimentam o campo em cinco blocos.

A interpretação sísmica foi realizada com o apoio tanto dos dados de amplitude quanto os de impedância acústica. O dado sísmico utilizado nesse estudo data da década de 80, época em que grande parte dos poços já haviam sido perfurados. O processamento do mesmo foi encerrado no ano seguinte, com a seguinte parametrização:

- Dimensão da cela: 25 m x 33.33 m;
- Deconvolução de fase da onda – mínima;
- Deconvolução pré-stack – fase mínima;
- Equalização RMS de amplitudes;
- Migração por diferenças finitas;
- Deconvolução pós-stack – fase zero;
- Filtro 6/18 – 65/48 Hz./dB/oitavas.

A impossibilidade de reprocessamento desses dados de acordo com parâmetros mais atuais e voltados para a interpretação em escala de reservatório maximiza o desafio do trabalho.

Metodologia

Foram as seguintes as etapas do trabalho:

- **Interpretação preliminar**, com o rastreamento dos refletores regionais e da base do reservatório.
- **Conversão Tempo-Profundidade**, com o emprego de métodos geoestatísticos.
- **Inversão sísmica** acústica, considerando modelo inicial regional e método estatístico.
- Interpretação de seções geológicas e refinamento do seqüenciamento estratigráfico dos perfis, com suporte do dado sísmico de amplitude e impedância.
- **Interpretação sísmica de detalhe**, com suporte do dado invertido e das seções geológicas pré-interpretadas.
- Inversão sísmica acústica, considerando modelo inicial refinado.
- Ajuste na conversão Tempo-Profundidade, corrigindo pequenas variações no posicionamento estratigráfico e acrescentando pontos internos ao reservatório.
- Ajuste final da interpretação sísmica, considerando os dados reinvertidos.

Interpretação Sísmica preliminar

Essa etapa, efetuada de modo expedito, foi importante para as etapas posteriores de preparação dos dados, tendo sido interpretados os horizontes guias dos processos de conversão para profundidade e inversão sísmica. Também foram traçadas as principais estruturas delimitadoras do reservatório.
Foram interpretados: Topo do Eoceno-250, Topo do Quissamã e a base do reservatório, todos com forte expressão sísmica. A base do reservatório representa a principal feição observada no campo, sendo representada por um forte pico de amplitude positiva, correspondendo ao contraste do mesmo com as seqüências carbonáticas inferiores.

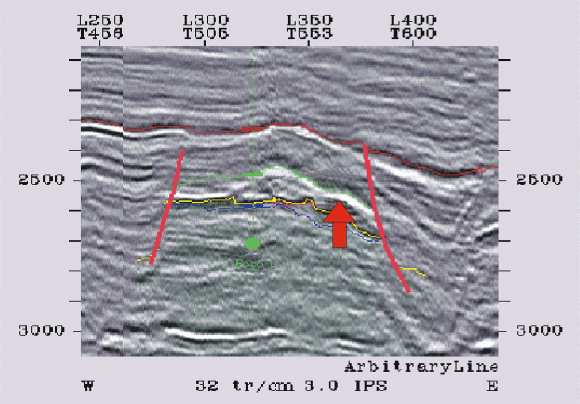

Figura 1 – Seção sísmica em tempo. Notar refletores regionais e falhas delimitadoras. Reservatório representado por anomalia branca na seção.

Conversão Tempo-Profundidade

O modelo de velocidade empregado na conversão foi calculado com o emprego de métodos geoestatísticos, consistindo em uma Krigagem com deriva externa entre os pontos de amarração sísmica (em tempo) e perfis (em profundidade).
A deriva externa foi definida a partir dos dados de perfis sônicos, devido à inexistência dos arquivos de análise de velocidade. Foram utilizados os horizontes regionais para guiar a interpolação.

Inversão Sísmica

A obtenção do modelo ótimo de impedancia acústica deu-se com o emprego de procedimento com formulação baysiana, no qual os dados de amplitude são ajustados a um modelo de impedância acústica inicial, gerado a partir de informações derivadas de poços e do conhecimento geológico prévio.

As etapas desse procedimento podem ser agrupadas em:

- Determinação da wavelet (integração perfil-sísmica).
  Foi considerado como o melhor ajuste, uma wavelet de fase zero, de comprimento igual a 204 ms, correspondendo a um filtro de Hanning, com freqüência de corte 0-8/40-60 Hz.
- Geração do modelo a priori (condicionamento inicial da inversão).
  Foram utilizados 18 poços, representando todos aqueles com perfil sônico na área de estudo.
  O modelo da primeira inversão efetuada considerou como condicionantes a Base das areias e o topo do Eoceno-250. Já para a segunda inversão, a esses dois horizontes somaram-se o topo da Seqüência 1 e o topo do Cenomaniano-150 (Figura 2).
- Inversão propriamente dita.

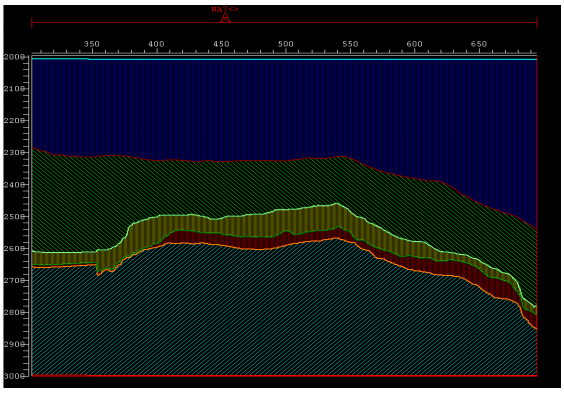

Figura 2 – Modelo geológico da Inversão II

Estratigrafia/ Modelo Deposicional e Interpretação Sísmica de Detalhe

No modelo estratigráfico estabelecido para o reservatório foram definidas duas seqüências de terceira ordem, sendo a inferior dividida em três subseqüências de quarta ordem (seqüências 0, 1 e 2) e a superior em duas (seqüências 3 e 4).
Os eventos de terceira ordem são controlados por movimentação tectônica, principalmente halocinese e eustasia. O primeiro evento, com cerca de 4 ma e datado do Albiano superior, está depositado sobre seqüência carbonática, em calhas criadas, principalmente, pela a ação da tectônica do sal.
O segundo evento, de idade Cenomaniano médio, foi depositado em um periodo pouco maior que 4 ma de anos, após um hiato de 2.4 ma, reconhecido em seções sísmicas, análises bioestratigráficas e perfis de poços. Comparativamente ao evento sotoposto, possui caráter menos confinado**.**
Do ponto de vista deposicional, as cinco seqüências de quarta ordem podem ser agrupadas em três sistemas turbidíticos distintos.
O primeiro envolve a Seqüência 0, que representa a porção mais basal do reservatório. A deposição dessa é relevante apenas na porção S/SE do campo, possuindo forte controle tectônico. Os sedimentos dessa são constituídos, em sua maior parte, por depósitos de escorregamento e fluxo de detritos, além de isolados depósitos turbidíticos confinados.
Como pode ser visto nos histogramas da figura 3, comparativamente às seqüências superiores, a Seqüência 0 possui valores de impedância mais eleva-

dos, correlatos às fácies não reservatório. No dado sísmico esse contraste é bem pronunciado, o que facilitou o mapeamento do topo dessa seqüência. A figura 4 apresenta o mapa de espessura sísmica dessa unidade,.

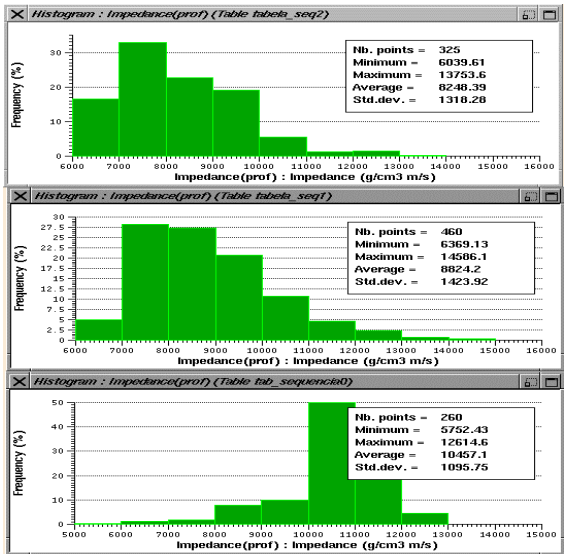

Figura 3 – Histograma de impedâncias das seqüências 0, 1 e 2. Notar a boa discriminação da Seqüência 0, em relação às superiores.

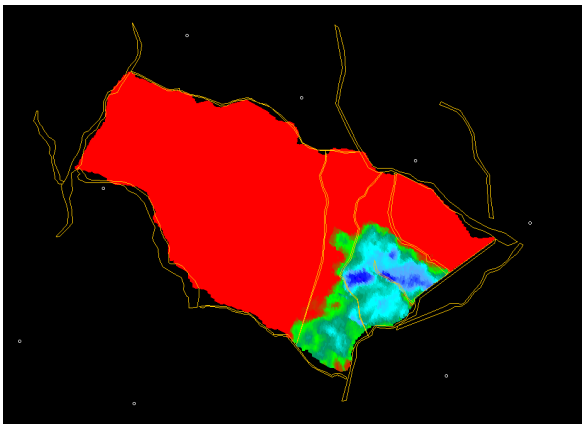

Figura 4 – Mapa de espessura sísmica da Seqüência 0. Notar forte controle estrutural.

O segundo sistema turbidítico engloba as seqüências 1 e 2. O controle tectônico continua a ser preponderante na geração de espaços para a deposição, principalmente na criação de uma calha contínua, onde se deposita a Seqüência 1 (Figura 5). A Seqüência 2 é depositada em duas calhas menores (Figura 6). A separação entre essas duas seqüências é possível devido ao comportamento sísmico da zona de condensação do topo da Seqüência 1, posicionada em pico de amplitude positiva.

No dado sísmico de amplitude não existem feições que possibilitem o rastreamento do topo da Seqüência 2. No entanto, apesar da pequena diferença entre os valores de impedância dessa seqüência e os da Seqüência 3 (Figura 7), foi possível a interpretação nesse tipo de dado, uma vez que as feições geométricas observadas mostram coerência com os marcos estratigráficos observados em perfil.

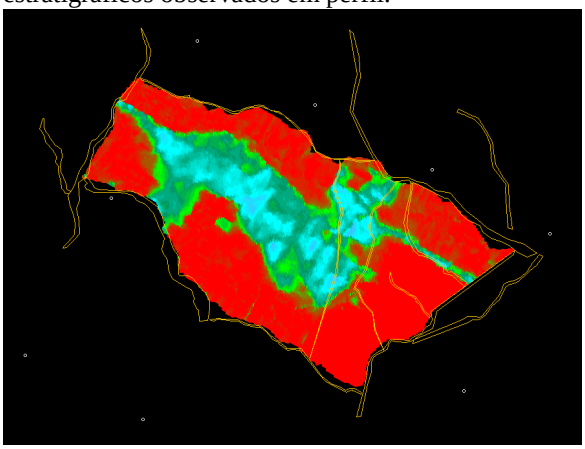

Figura 5 – Mapa de espessura sísmicada Seqüência 1. Notar deposição confinada à calha principal.

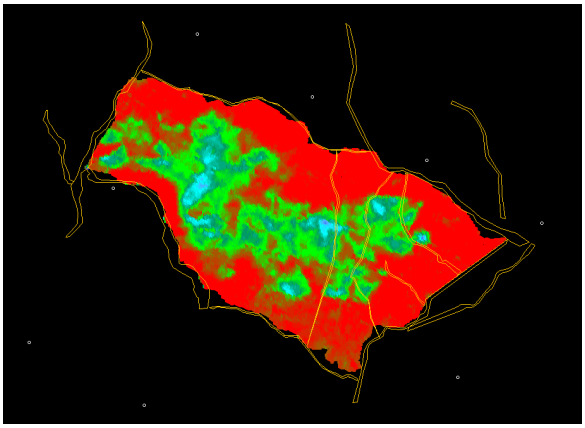

Figura 6 – Mapa de espessura sísmica da Seqüência 2.

O terceiro sistema turbidítico engloba as seqüências 3 e 4. O hiato erosivo entre esse sistema e o sotoposto, de pequena expressão no dado de amplitude sísmica, é corretamente identificado no dado invertido para impedância acústica, onde são observadas as estruturas se interrompendo na discordância entre os dois sistemas (Figura 8).

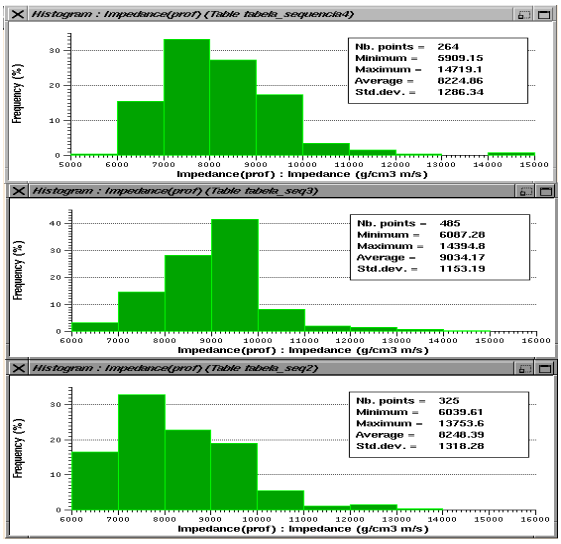

Figura 7 - Histograma de impedâncias das seqüências 2, 3 e 4.

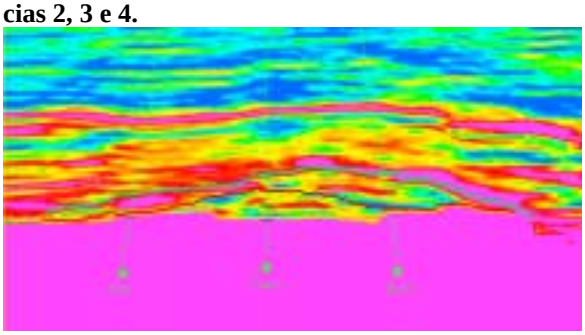

Figura 8 – Seção em impedância acústica. Notar as feições geométricas contra o refletor assinalado – Topo da Seqüência 2).

As seqüências desse terceiro sistema são depositadas de maneira mais espraiada. A inexistência de uma zona de condensação pronunciada no topo da Seqüência 3, além do posicionamento das impedâncias das duas seqüências na mesma faixa de valores, impede a compartimentação desse sistema com base do dado sísmico (Figura 9).
O pacote é recoberto por um espesso pacote de lamitos radioativos, identificados na sísmica, e que representam o topo do reservatório.

Conclusões

A base de dados sísmicos utilizados, adquirida há 15 anos e impossibilitada de ser reprocessada, pode ser vista com um fator limitante de qualidade no presente trabalho. Algoritmos mais recentes de processamento, que buscam uma maior acurácia na preservação das amplitudes sísmicas, certamente gerariam uma maior confiança nestes como dado de entrada para os aplicativos de inversão estratigráfica. Do mesmo modo, uma maior resolução na aquisição dos dados ocasionaria uma maior definição das feições internas ao campo.

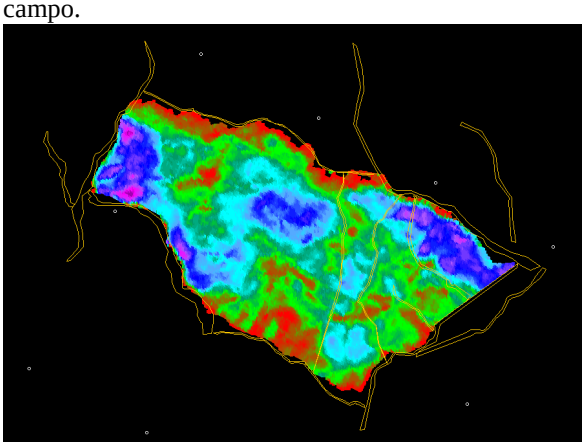

Figura 9 – Mapa de espessura sísmica das seqüências 3 e 4. Notar o maior espraiamento do reservatório.

A metodologia aplicada na conversão tempo–profundidade foi idealizada durante a realização do projeto, visando contornar a inexistência de dados de análise de velocidade de empilhamento nos bancos de dados da companhia e, pelos resultados apresentados, poderá ser aplicada em situações similares.
A interpretação dos limites do reservatório foi efetuada, de maneira satisfatória, tendo como base o dado de amplitude sísmica, no entanto, algumas das seqüências internas desse, que tiveram seu posicionamento balizado pelos dados de bioestratigrafia, só puderam ser definidas na sísmica baseadas na impedância.

Referências Bibliográficas-

Johann, P., 1997, Inversion Sismostratigraphique et Simulations Stochastiques em 3D: Réservoir Turbiditique, offshore du Brésil. Intègration Geólogique, Géophysique et Géostatistique. Tese de doutorado, 351 pp.

Schwedersky, G., Mundim, E.C. e Johann, P, 1999, Inversão Sísmica na Caracterização de Reservatório. Relatório Interno, Petrobras, 65 pp.

Mundim, E.C., 2000, Conversão Tempo- Profundidade. Relatório interno – Petrobras, 49 pp.

Agradecimentos

Agradeço à Petrobras por permitir a publicação desse trabalho e também aos geólogos Rosane Trajano, Eduardo Rodrigues, Viviane Santos e Oscar Strohschoen pela definição de todo o arcabouço geológico, base para esse trabalho. Agradeço também aos geofísicos Paulo Johann, e Evaldo Mundim pelo pioneirismo e apoio nos procedimentos aqui relatados.

Sedimentary facies mapping based on bottom surface backscattering strength

Maria Gilda P. Esteves LAGEMAR-UFF, Brazil (gilda@igeo.uff.br); *Alberto G. Figueiredo Jr. LAGEMAR-UFF, Brazil (alberto@igeo.uff.br)* and *Letícia R. de Carvalho* FURG*, Brazil (doclrc@super.furg.br)*

Abstract

Bottom surface backscattering strength (BSBS) data from southern Brazilian shelf and slope, between Cape São Tomé and Arroio Chuí were used to characterize bottom sediment from 50 to 1,500 m water depths as part of the Brazilian national program entitled "Sustainable Potential of Living Resources of the Economic Exclusive Zone" (REVIZEE). The BSBS data is compared to 3,036 bottom samples and results allowed bottom sediment classification accordingly acoustic characteristics and grain-size.

Introduction

Mapping of sedimentary facies and depositional processes at the ocean bottom based on response to echo sounders (echo character) have been applied by Damuth (1975), Mullins *et al.* (1979), Flood (1980), Costa (1997) and Costa & Figueiredo Jr. (1998). And since development of digital technique for storing echo sounder data, it has been possible to associate level of acoustic impedance to sediment facies. This technique was applied to an area of the Brazilian continental shelf and slope between Cape São Tomé and Arroio Chuí in an extension of 2,400 km in water depths ranging from 50 to 1500m. This mapping was developed as part of a Brazilian national program entitled "Sustainable Potential of Living Resources of the Economic Exclusive Zone" (REVIZEE) on board of RV Atlântico Sul from Fundação Universidade Federal do Rio Grande (FURG).

The authors are aware of software packages able to used BSBS to classify ocean bottom sediment, however due to high commercial costs of packages and possibility of development of the technique inhouse, we decide to write this paper.

The Data Set

The acoustic data were collected with a Simrad EK 500 echosounder operating in a frequency of 38 kHz. The data used is one of the acoustic measurements provided by the echosounder telegram called "bottom surface backscattering strength (BSBS). The values are furnished in decibel and were collected in a rate of 9 to 12 values per minute with ship sailing at 10 knots.

Bottom sample data are from 3,036 samples from the Brazilian Program in Marine Geology and Geophysics (PGGM) Data Bank, from the Brazilian Margin Reconnaissance Program (REMAC) and REVIZEE Program.

Bottom Classification Procedure

In order to proceed with sediment classification, initially the sediment samples have to be classified accordingly to Shepard (1954) triangular diagram of proportional mixing of sediment types (Fig. 1).

Next, sample class is compared to BSBS values having as common data the geographical coordinates.

For sediments in the extreme of the classification diagram, BSBS values are well defined, but in many cases of sediment mix, BSBS values could correspond to more than one sediment class. In these cases, decision has to be taken, based on statistical occurrence and better fitting of the data.

Results can be used as bulk values of decibel X sediment class or transformed into maps were areas of same BSBS values are contoured.

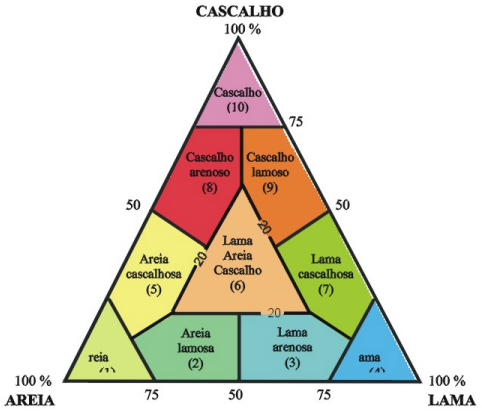

Figure 1 –triangular diagram of mix proportion of sediment. (After Shepard, 1954)

Results

Correlation of sediment class to BSBS values have shown that BSBS values can belong to more than one sedimentary class, depending on the mixing of sediment percentiles. Taking into account this consideration, sediment classes can be grouped in four BSBS levels as indicated in table 1.

Table 1. Classification of sediment mix accordingly their response to backscattering strength.

Backsattering Strength Level (dB)	Sediment Mix Classification Accordingly to Shepard's Diagram
-05 to -10	gravel; muddier gravel; sandier gravel; gravel/sand/mud; gravelly sand and sand.
- 10 to -15	Gravelly mud; sandier mud; muddier sand and sand
- 15 to - 20	muddier sand and mud
< - 20	mud

Application of the technique to a cross-section of continental shelf and slope has shown that there is a good correlation between sediment class and BSBS and that BSBS is independent of water depth (Fig. 2). A detailed description of procedures and results can be found in a REVIZEE internal report by Figueiredo Jr. *et al.* (1999).

Once established a correlation pattern for a specific area, sediment class can be also inferred based on BSBS values. Application of the technique to an area of continental shelf and slope of Rio de Janeiro and São Paulo State have identified that sandier sediments covers larger extension the outer shelf with some isolated coarser sands and gravel (Fig. 3). Close to Cabo Frio and southwest of Rio de Janeiro, the percent of muddier sediment increases with BSBS values varying between -15 to -20 dB. The same situation can be seen on the slope were BSBS values are inferior to -15 dB.

Conclusions

Correlation BSBS values with sediment classes has proved to be an inexpensive and expedite tool for mapping transects and large areas as first approach prior to further investigation.

Because several variables can influence the BSBS values the more samples available; the better are the results.

Acknowledgments

The authors are thankful to Prof. Lauro Saint Pastous Madureira and his assistant Rafael Agrello Dias from FURG for their valuable help during execution of this work. We are also grateful to REVIZEE coordinators for supporting our research. The Brazilian National Research Council (CNPq) sponsors Alberto G. Figueiredo Jr. in his research.

References

Costa, E.A., 1997, Caracterização de ecofácies e processos sedimentares da plataforma continental amazônica: MSc. Thesis, Fluminense Federal University, 138pp.

Costa, E.A. and Figueiredo Jr., A.G., 1998, Echo-character and sedimentary processes on the Amazon continental shelf, Anais da Academia Brasileira de Ciências, 70, (2), 187-200.

Damuth, J.E., 1975, Echo character of the Western Equatorial Atlantic floor and its relationship to the dispersal and distribution of terrigenous sediments. Marine Geology, 18, 17-45.

Figueiredo Jr, A.G. and Madureira, L.S.P., 1999, Programa de Avaliação do Potencial Sustentável de Recursos Vivos na Zona Econômica Exclusiva – REVIZZE. Relatório Final dos dados Geológicos, 58 pp.

Flood, R.D., 1980, Deep sea sedimentary morphology: modeling and interpretation of echo-sounding profiles. Marine Geology, 38, 77-92.

Mullins, H.T., Boardman, M.P. and Newman, A.C., 1979, Echo character of off-platform carbonates. Marine Geology, 32, 251-268.

Shepard, F.P. (1954). Nomenclature based on sand-silt-clay ratios. Jour. Sed. Petrology 24, p. 151-158.

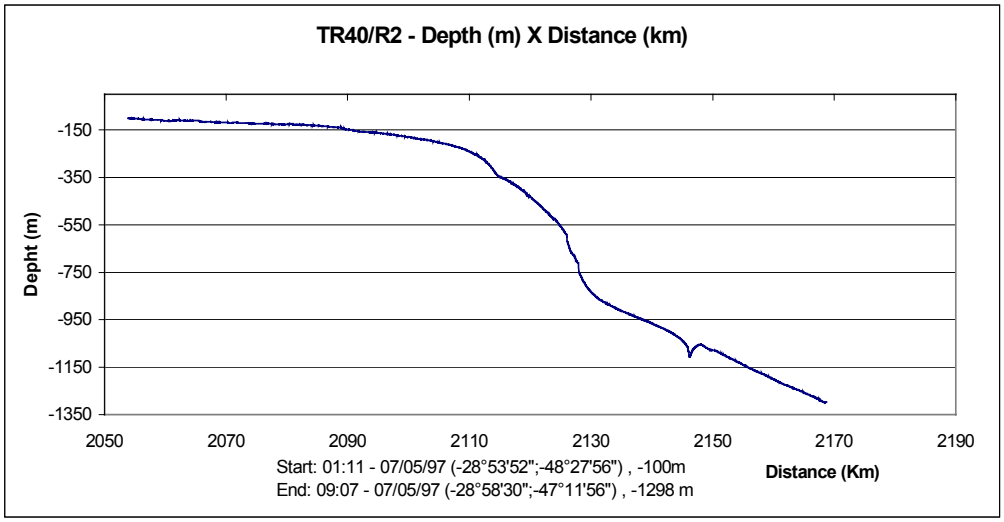

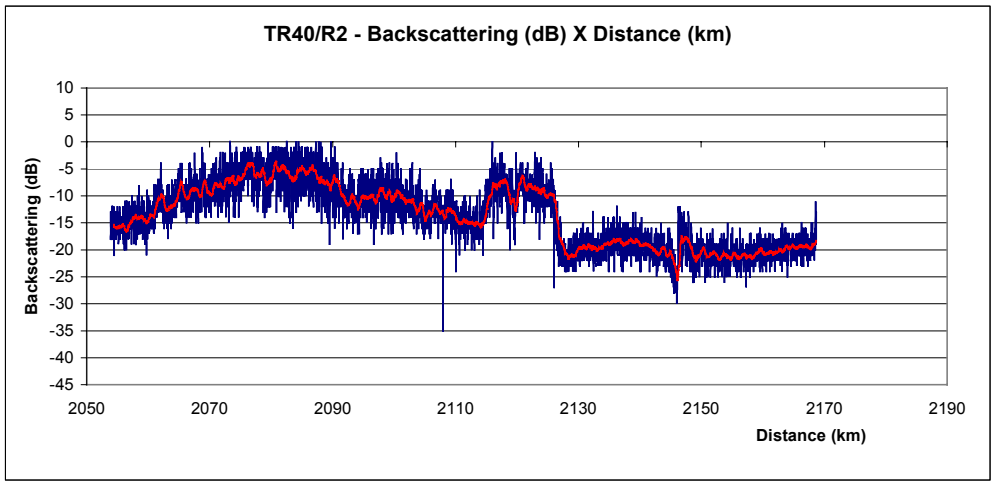

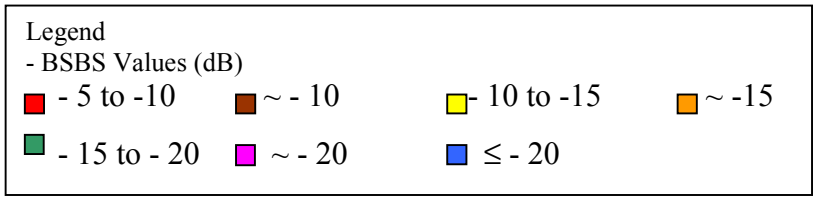

Figure 2 - Continental shelf and slope cross-section showing bottom topography, BSBS values with mobile mean (center line) and sediment class.

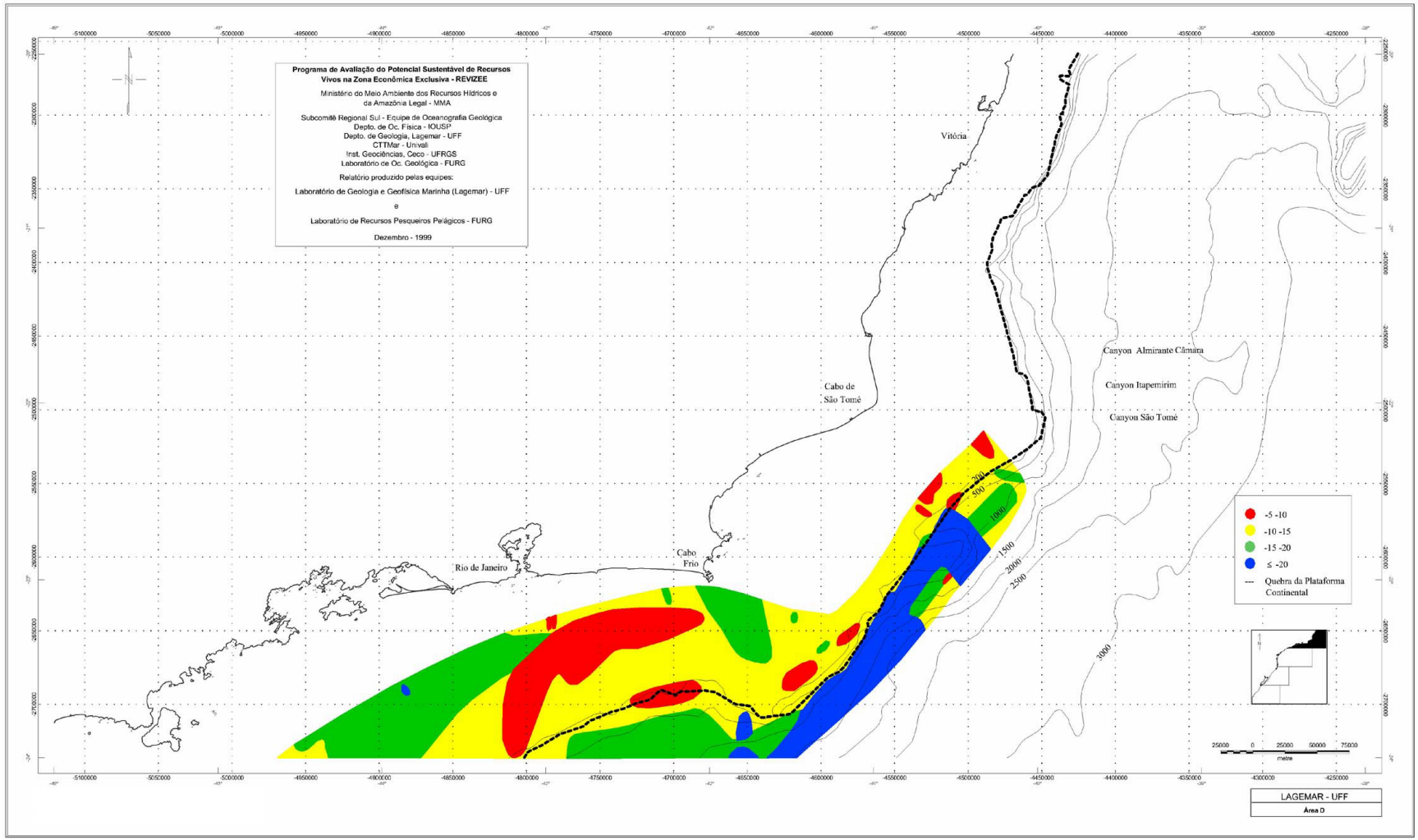

Figure 3 – BSBS map based on dada from a Simrad EK 500 echo sounder (data source REVIZEE Program).

Seismic Data @ccess: Managing the Propagation of Pervasive Volumes

Jess B. Kozman, Schlumberger Oil & Gas Information Solutions, Houston, TX; Ken Hauser, GeoQuest, Lagos, Nigeria

Abstract

Successful seismic data management solutions are combinations of hardware, software, and onsite services to provide integrated, vendor-neutral, open-systems solutions. They are implemented to add value to the interpretation environment and designed by geoscientists for use by oil industry professionals. The solutions are scalable to enable automatic data management and immediate/transparent data access, which optimizes the seismic data management environment. The goal is to provide a collection of tools and processes that efficiently deliver exploration data to the desktop. The solution should enable the management of seismic data from design of a survey through the divestiture of the project.

Why a seismic data management solution?

Among the fundamental problems that occur when a comprehensive seismic data management solution is not in place are the inability to identify, locate, and access data, and insufficient disk space for data storage.

In many organizations, interpreters are unable to fulfill the basic operational need of generating a map that shows all the seismic data that is available online. Value can be lost when a company purchases the same data multiple times or is unable to identify overlapping ownership during a merger, acquisition, or joint ventures. When data is not delivered quickly and efficiently the time spent looking for data increases and directly competes with the core business of exploration. These inefficiencies can be measured in longer times to payout, increased project cycle times and decreased barrels of oil produced per geoscientist.

The second problem that occurs without a seismic data management solution is the lack of disk space for data storage. There has been a tremendous increase in the number of versions of a seismic volume that geoscientists are able to generate using workstation tools in the interpretation process. This increase is driven by technologies such as visualization, attribute analysis, and iterative migration. Production requirements can demand reshoots of existing seismic data to utilize seismic timelapse monitoring techniques, leading to multiple chronological versions of the same survey geometry being interpreted simultaneously. In the prestack domain, Amplitude Vs. Offset (AVO) format data, prestack depth-migration data, and three-component seismic data already are in use and are likely to become more standard. Other interpreter created volumes include depth ,variance, flattened, time-slice and surface-slice. Case histories indicate an exponential growth of seismic volumes in the interpretation environment. This leads to pressure on disk storage and backup infrastructure.

New interpretation tools will continue to develop and will generate additional seismic trace data or new volumes as output. In turn, this will require that significant disk space be available or will require significant changes to current practices of seismic data management. Oil and gas exploration company's core competency is finding oil and gas, and more and more they are turning to data storage solution providers to insulate them from the step-changes in technology required to maintain efficient seismic data access.

What is a seismic data management solution?

A seismic data management solution has two distinct elements—a Geographic Information System (GIS) based data catalog and a disk/tape management system. There is an expectation in most organization that a geotechnical professional should be able to view a map, drag and drop a spatial area of interest and be presented with a searchable listing of all of the seismic volumes that are available. This interface provides views of the data, access to project metadata, and automatic loading of industry-standard delivery formats to target applications. The disk/tape management system enables hierarchical storage management (HSM) techniques and tape robotic storage of aged data nearline and enable organizations to manage the explosive growth of seismic data volumes that are required in the interpretation environment. As new and beneficial interpretation techniques are implemented, these data management tools will seamlessly administer the movement of resulting seismic volumes between online, nearline, offline and offsite environments.

Together, these technologies suggest a new paradigm in seismic data management—real-time access to data, state-of-the-art management of all seismic data volumes generated during the interpretation processes, and the treatment of seismic data as a corporate asset that must be protected and managed.

User Interface

The GIS interface to a seismic data management system creates a working, up-to-date catalog of an organization's seismic data by creating a link via a spatial catalog between project metadata and the related seismic trace data either in native format or in a variety of interpretation formats. Physical copies of the bulk trace data are not duplicated in this catalog, but stored online in file systems using Network Attached Storage (NAS) or Storage Area Networks (SAN) to leverage high-speed delivery to applications. Scanning tools are provided to continually update and verify the data storage environment as new volumes are added, and the catalog must be HSM aware so that a catalog can be maintained whether data is online, nearline, offline, or offsite.

The best way to see accessible data is via a map and a logical hierarchy implicit in the tables generated by the interface. This structure would be:
project table – names of projects in applications or directory structures
navigations table – master grids of 3d data or shot-to-trace relationships for 2d
section table – listing of multiple versions of the same trace file
Users are able to point and click to select items in any table or on the map view and see the many-to-many relationships between projects, navigations and multiple trace files that are maintained in the database (Figure 1).

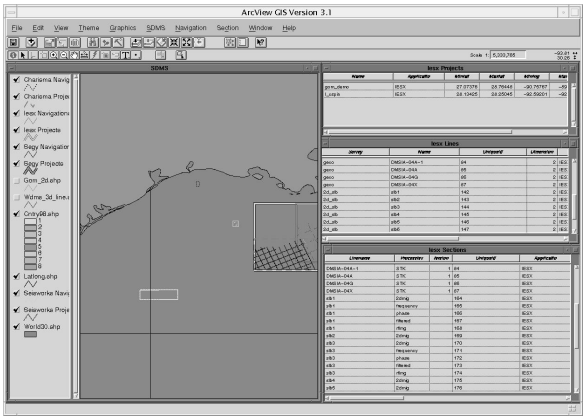

Figure 1. The GIS interface shows a map with project table, line table and section table.

Additional modules give complete control over the seismic data management environment with reports, quality control routines and updating procedures. A seismic data loader cleans, conditions and loads seismic data into a corporate seismic database, with the ability to examine and edit line and trace headers, analyze amplitude and spectral characteristics, apply scaling and clipping, merge with navigation files, and subset, filter, or phase rotate the data when loading to applications (Figure 2).

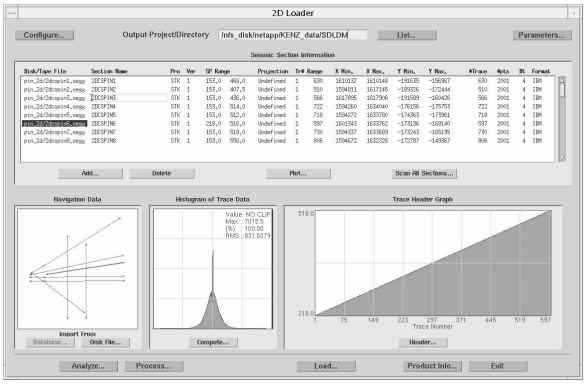

Figure 2. The seismic data loader shows navigation plot, amplitude histogram and trace header plot for selected line.

A seismic trace viewer is provided to QC trace data prior to loading the selected data from the corporate SEG-Y datastore into the project environment. Standard file format templates are available—or new templates can be created—to establish and maintain corporate standards for line and trace header information, survey data and associations to external files.

Finally, the catalog should allow the association of other user-defined data types—such as text, pictures, project archive information—with a line or section.

Disk Tape Management

Behind the scenes, a suite of software and hardware products enables the implementation of the HSM element of the seismic data management solution. HSM allows seismic data volumes that meet client-specified business rules to be transferred from the online disk environment and stored on tape in the robotic tape library. This frees up space for continuing interpretation activity. File usage is tracked by access dates and modify dates as registered in the inode. Data is available on demand, but the

system administrator no longer is required to continually add new online disk capacity. As seismic data volumes age in an interpretation project they are accessed with less frequency (Figure 3).

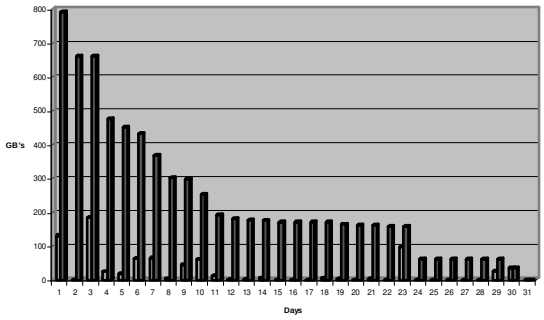

Figure 3: Graph showing the amount of data in a typical interpretation environment which can be released after a number of days of non-access.

When these volumes have not been accessed for a specified period, they can be moved to nearline tape storage. This frees up valuable online disk space and expedites backup procedures; because the seismic data volumes are on tape they no longer require nightly backups. Backup processes that once took hours, but now take entire weekends, can be reduced back to hours.

While there is an assortment of commercially available hardware/software combinations that facilitate such a solution, the model generally is the same. Standard HSM technologies support the automatic movement of seismic data volumes from costly online disk locations to less expensive nearline tape storage media as the data ages within client-specified business rules. These same technologies automatically migrate the data back online at user or application request. When a new seismic volume is created or loaded on the file system, HSM identifies the volume as a new addition and a copy immediately is made to the nearline tape library. The HSM can be configured to make one copy nearline and one to be removed for disaster recovery. After a specified period of time during which the online file has not been accessed (an example would be a business rule set at 90 days), the file becomes a candidate for release from the online disk system.

Once the online disk environment reaches a client-specified capacity, there is competition for online disk space among user groups. Candidate files meeting the age or size criteria or weighted by combinations of attributes are released from online disk and resides only nearline. A pointer to the tape address replaces their location. If a data file is requested after it has been released from the online environment, an automatic retrieval process is invoked and the data are transferred from nearline back to online disk for immediate access. In this scenario, online disk space automatically is managed between client-specified high and low thresholds without the need to continually add new disk space. Tape copies of all files are made automatically and are available for disaster recovery scenarios.

Innovative hardware installations are required to store, track, deliver and archive enormous seismic volumes during a project's life. Massively expandable robotic mass-storage tape repositories that store terabytes or petabytes of data are available commercially. These hold multiple tape cassettes, each capable of storing 200 gigabytes of uncompressed data. The robots contain tape drives that support sustained throughput of 24 megabytes/sec, and accelerate the delivery of tapes to tape drives and nearline information to the desktop. Daily project backups are simplified by ignoring the large seismic data volumes because they are on tape; the timeframe for completion is compressed. Third-party project archiving makes final archiving simple and retrieval of archived information robust and efficient (Figure 4).

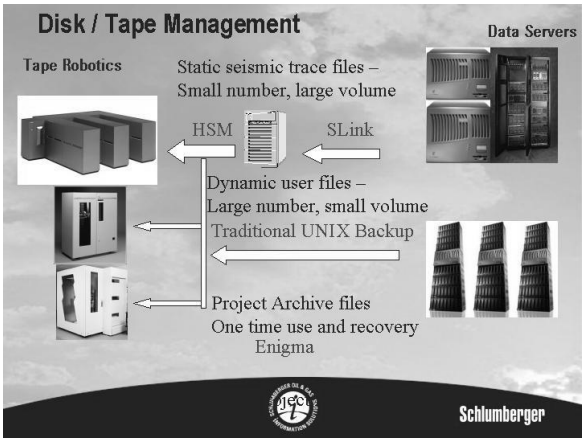

Figure 4: A fully functional disk/tape management system, showing the most efficient handling of different data types in an interpretation environment

Seismic @ccess

Summary

A seismic data management solution is a combination of hardware and software that can be integrated into the workflow of any exploration company. The solution can be configured for existing architecture or hardware recommendations can be made for new installations. A flexible and powerful data management tool is a proven solution to meet expanding seismic data management needs.

Seismic Stratigraphic Interpretation of Salt Minibasins, Gulf of Mexico, USA

Alexandre Santos de Castro, PETROBRAS S/A, Brazil

Abstract

Gulf of Mexico basin is one of the most intensely studied sedimentary basins in the world, especially because of its important petroleum province. This basin is also known because of its complex interplay of salt tectonics and sedimentation and related deep-water turbidite deposits.

It is presented in this paper the partial results of seismic stratigraphic interpretation using 3D seismic data and well log profiles in an integrated approach. The selected area is located at outer shelf and upper slope of Ship Shoal and Green Canyon areas, offshore Louisiana. The studied sediments were deposited in slope and deep water settings under very high deposition rates and salt related minibasins.

Seismic depositional sequences were identified from 5.8 Ma (Upper Miocene) to Present, using the basic principles of seismic and sequence stratigraphic techniques.

A mathematical modeling for spatial representation of stratigraphic surfaces is presented. This technique aims to a better representation of seismic stratigraphic elements.

Seismic Stratigraphic Studies

Seismic stratigraphy is a very important tool for petroleum exploration, and it is becoming more popular with the increasing quality of seismic data and the spreading of 3D seismic acquisition in most of sedimentary basins worldwide. The basic principles of this technique were proposed by Exxon explorationists (Vail *et al*., 1977), and state that within the limits of seismic resolution (and considering some possible exceptions) seismic reflections follow gross bedding and such they approximate time lines. Therefore a seismic section can be assumed to carry chronostratigraphic information as well lithostratigraphic information derived from reflection characteristics at acoustic impedance contrasts.

In this study, seismic analysis of several minibasins in Gulf of Mexico are presented with the data tied to the wells to produce logical environmental interpretation of the data.

Several seismic depositional sequences were identified and classified by external and internal characteristics.

Figure 1 shows an example of seismic profile of the study area where it is possible to identify the important seismic stratigraphic sequences. The ages were defined using biostratigraphic (planktonic foraminifera and calcareous nannofossil) information

The use of seismic attributes such as amplitude, frequency or continuity can be very important to identify depositional features. Figure 3 shows a continuity time slice taken at 500 milliseconds below sea level to show the richness of information of modern seismic data. It is possible to identify in that picture the main sedimentary areas, salt bodies as well to easily interpret areas with fault occurrence.

Most of studied minibasins present subparallel seismic facies (typical of deep water settings), with common chaotic deposits (slumps and slides close to salt diapirs).

Salt Tectonics vs. Sedimentation

Sedimentary loading drives salt mobilization, which in turn affects the shapes of passive diapirs and allochtonous salt sheets in an interactive and complex interplay.

An important structural feature in Gulf of Mexico architecture is the presence of depositional minibasins caused by salt flowage and high rates of sedimentation. These minibasin are exploration targets and may be visualized even in the modern sea floor surface. Figure 2 represents a bathymetric map with the location of the studied 3D seismic data.

Rowan *et al*.(1995), and Schuster *et al*. (1995) present evolutionary models of salt minibasin formation from initially undeformed salt stocks and salt sheets evolving to salt / sediment systems. The final models are named Roho Stepped Counter Regional and Bowl-shaped systems. In all the cases salt downbuilding (passive diapirism) is the main process of salt body growth. In the study area Roho and Bowl-shaped minibasins are observed.

Mathematical Modeling of Stratigraphic Surfaces

For a better understanding of the relation between the key stratigraphic surfaces (i.e. unconformities, condensed sections) a mathematical modeling is being developed in Petrobras Research Center. This algorithm aims to represent the real relationship between the surfaces that define external and internal geometric features and allows a better interpretation of the sequences, systems tracts and depositional environments.

Conclusions

It is reviewed in this work the fundamentals of seismic stratigraphy and its applications of reservoir exploration in areas of salt tectonics, and the depositional geometries present in slope minibasins of offshore Gulf of Mexico.

The study was based on the integration of 3D seismic data and well log profiles and biostratigraphy, and a detailed seismic facies analyses is presented.

Modern salt/sedimentation models are discussed, with application in the study area.

References

Diegel, F.A., J.F. Karlo, D.C. Schuster, R.C. Shoup and P.R. Tauvers, 1995. Cenozoic structural evolution and tectono-stratigraphic framework of the northern Gulf Coast continental margin. In*:* M.P.A Jackson. D.G.Robertson and S.Snelson, eds*., Salt Tectonics: a global perspective,* AAPG Memoir 65, p.109-151.

Rowan, M.G., 1995. Structural styles and evolution of allochtonous salt, central Louisiana outer shelf and upper slope, In: M.P.A Jackson. D.G.Robertson and S.Snelson, eds*., Salt Tectonics: a global perspective*, AAPG Memoir 65, p.199-228

Rowan, M.G. and Weimer, P., 1998. Salt-sediment interaction, northern Green Canyon and Ewing Bank (offshore Louisiana), northern Gulf of Mexico. AAPG Bull., V.82, No.5B, p 1055-1082.

Schuster, D.C., 1995. Deformation of allochtonous salt structural systems, Eastern Louisiana Gulf Coast. In*:* M.P.A Jackson. D.G.Robertson and S.Snelson, eds*., Salt Tectonics: a global perspective*, AAPG Memoir 65, p.177-198.

Vail, P.R., Mitchum, R.M.Jr., Todd, R.G., Widmier, J.M., Thompson,.S.III,Sangree, J.B. Bubb, J.N. and Hatfeild, W.G., 1977. Seismic stratigraphy and global changes in sea level. In*: Seismic stratigraphy – Applications to hydrocarbon exploration.* C.E. Payton (ed.), AAPG Memoir 26, p.49-62.

Acknowledgments

The author would like to acknowledge Petrobras, University of Colorado at Boulder and Universidade Federal do Rio de Janeiro (UFRJ/COPPE) for allowing the opportunity of this doctorate research.

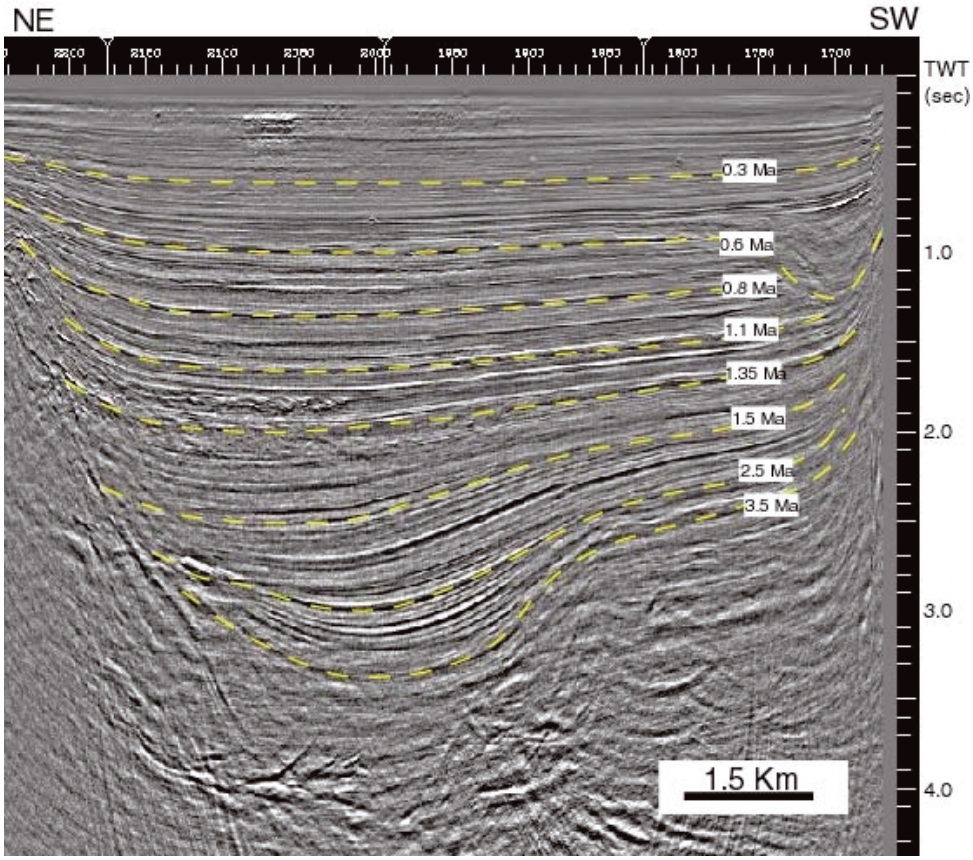

Figure 1 – Northeast–southwest seismic profile showing the interpreted seismic depositional sequences of a bowl-shaped minibasin. The actual configuration of salt diapirs are not clear in this image.

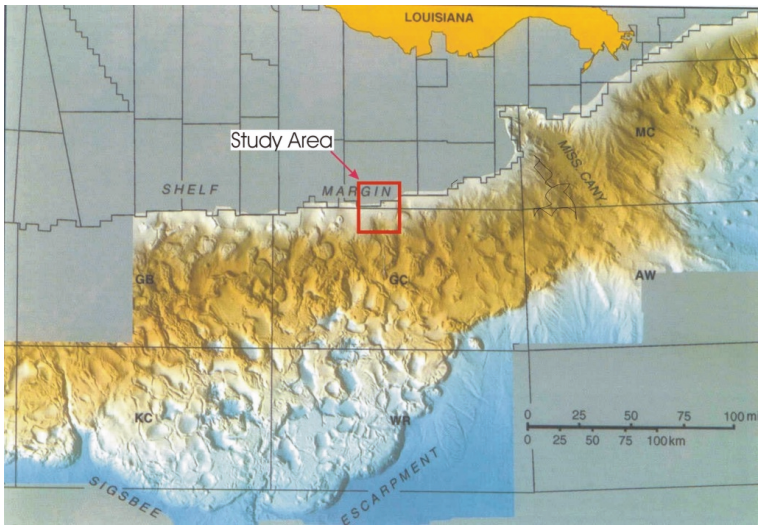

Figure 2 – Bathymetric map of Gulf of Mexico basin with the location of study area (from Diegel *et al*, 1995). It is possible to notice the existence of the salt-driven minibasins at the sea floor surface all over the continental slope.

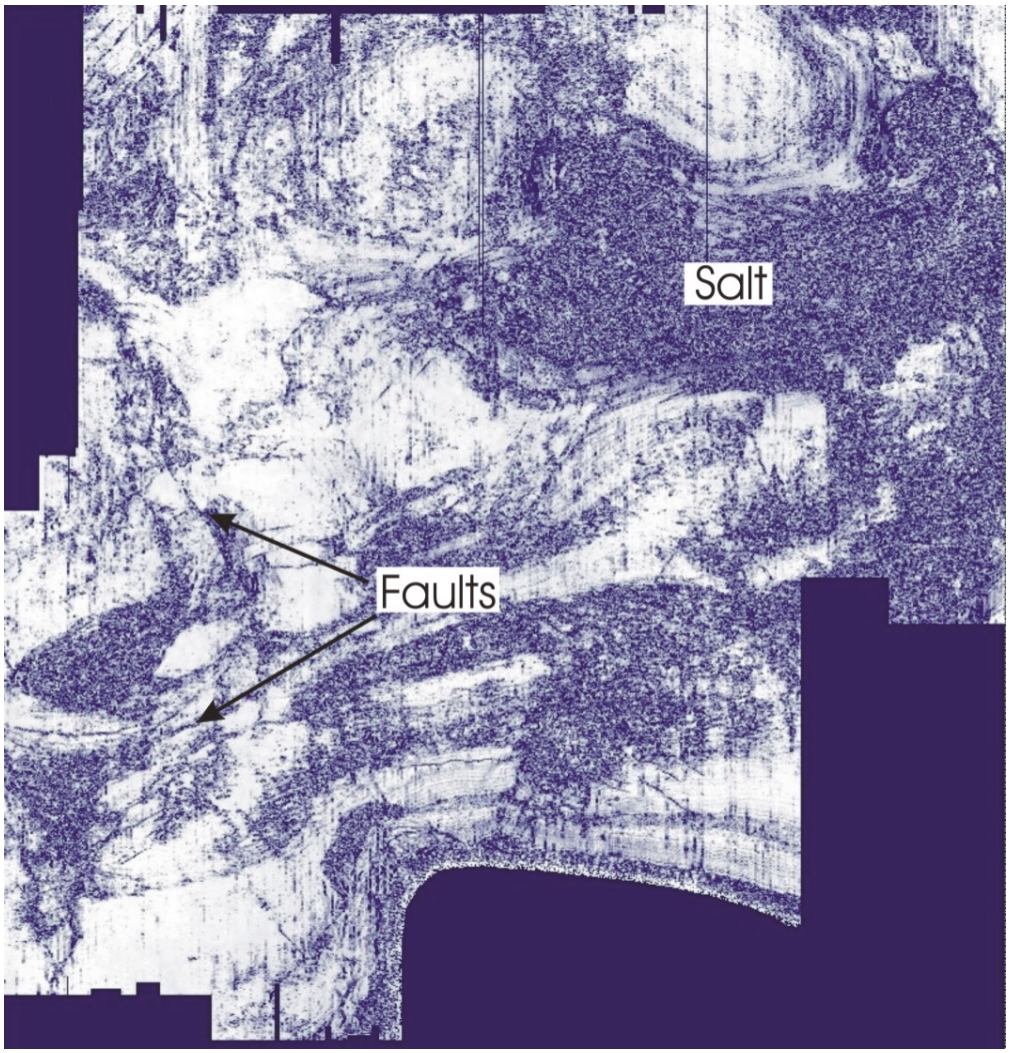

Figure 3 – Seismic time-slice of continuity data of the study area taken at 560 milliseconds. Lighter areas represent depositional minibasins and darker areas are salt bodies. Faults related to salt tectonics are also easier to identify in this kind of display.

Tectonics and Stratigraphy of East Java Sea North of Madura Island, Indonesia

Wisley de Oliveira Martins and Roberto Fainstein Schlumberger, Rio de Janeiro

Abstract

The purpose of this paper is to provide a modern regional geological and geophysical interpretation of the East Java Sea Basin. The basis for this seismic interpretation are 798 kilometers of recently acquired non-exclusive 2D seismic data and ties to well data.

The East Java Sea displays excellent examples of Miocene to present-day structural inversion of a back-arc Paleogene basin system. The structural geometry of these inversions has been analysed by a series of non-exclusive seismic surveys that demonstrate significant lateral variation in structural style.

Driving mechanisms of structural inversion have been assessed by modelling motions of the Eurasian, Indian Ocean, Australian and Pacific plates during the Neogene. The evolution of such inversion within the East Java Sea is interpreted as a function of the collision of the Australian Plate with the Sunda Arc. Moreover, the relative convergence rate and direction of the subducting Indian Ocean Plate and the S.E. Eurasian Plate affect inversion.

Two tectonic phases have been identified, one controlling the Paleogene rift and the other controlling the Neogene faulting

Structures formed during the Late Miocene were identified in seismic data. They represent prospective exploration features. On the shelf areas, patch reefs and shallow marine sandstone ranging from Oligocene to Middle Miocene are the targets for exploration. Reef limestones from the Pliocene age where sealed by Recent mudstones are also of interest.

Introduction – Non-Exclusive Survey

The East Java Sea Basin is part of back-arc basins that developed peripheral to the Sunda Shield, these extend from North Sumatra to Central Sulawesi. Onshore East Java is well explored and has been producing oil since the late 19th century. Exploration of the East Java Sea began in the early 1970´s and is a significant gas province. It is also have to currently sub-economic oil and gas finds.

Non-Exclusive Seismic Surveys have been conducted by Schlumberger WesternGeco since 1993 in all of the Souteast Asia Offshore Basins (Figure 1) with the aim of improving the petroleum geology knowledge of this area.

Modern data are now available on most of the offshore Tertiary Basins such as Palawan Basin offshore Philippines, Natuna Sea off Indonesia, Andaman Sea offshore Myanmar and North Sumatra, off Madura Island (Figure 2) and off North Bali in the East Java Sea Basin and in the Mahakam Delta/Makasar Strait region. In the Pre-Terciary Basins of the Eastern Indonesia and northwest shelf of Australia modern deep-water seismic data were also acquired and interpreted.

Figure 1: Location of non-exclusive 2D surveys undertaken in the Southeast Asia Archipelago by WesternGeco.

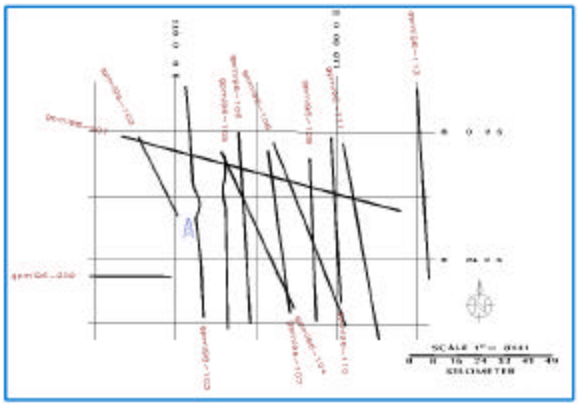

Figure 2: Location Map – Offshore North Madura Island Non-Exclusive Seismic Survey, East Java Sea.

Tectonic Setting

The sub-basins of East Java Sea are part of an extensive, complex, basin system that has developed around the margins of the SE EurasianPlate (Figure 3). The orientation of major fault zones defining these sub-basins boundaries varies around this margin. Three distinct trends are recognised. In the area of the Makassar Basin the main fault systems are orientated approximately NE-SW, parellel to the coastlines of East Kalimantan and West Sulawesi which form the flanks of the basin. Faults of this orientation continue SW into the East Java Sea where they define sub-basins such as the Masalima Trough, Central Deep and Muriah Trough. NW-SE trending faults are present within the Makassar Basin, notably north of the

Paternoster Plataform and offshore SW Sulawesi. The third major fault trend is best developed within the southern part of the East Java Sea, where sub-basins are defined by faults which trend approximately E-W.

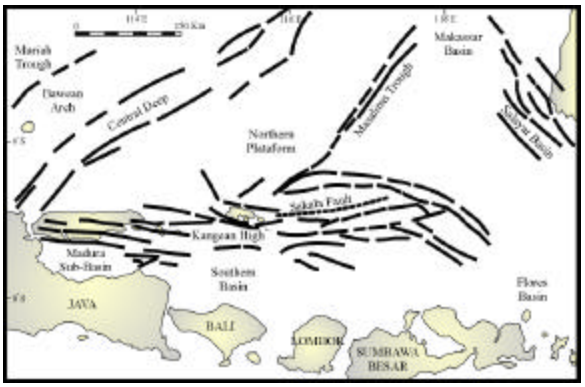

Figure 3: Southeast Sunda Shield basin distribution, showing orientation of principal structural lineaments.

The tectonic framework of this region results from motion of the Eurasian, Indian Ocean-Australian, and Philippine Sea Plates. Motion of the Indian Ocean plate is approximately towards the north and the Philippine Sea Plate approximately towards the WNW, both plates converging on the relatively stable Eurasian Craton. Convergence along the southern margin of the Eurasian Plate takes place by subduction of Indian Oceanic crust and by westerly propagating collision of the Australian continental crust with the island arcs to the north of the Sunda Trench. Along the eastern flank of the SE Eurasian plate convergence is accommodated by subduction of the Philippine Sea Plate.

Structural Geology

The East Java Sea Basin is embraced by four distinct tectonic provinces (Figure 4): (1) Platform Areas; (2) Central High; (3) Transitional Terraces and (4) Southern Basin. The Northern Platform areas are characterized by slow subsidence until the Miocene and mild inversion during Miocene-Pliocene. It compromises the Karimunjawa Arch, Muriah and Camar Trough, Bawean Arch, Bawean Trough, JS-1 Ridge (NE-SW trends), the Central Basin Inverted Graben and the North Madura Platform (a massive carbonate shelfal area during the Miocene and the Pliocene). The Central High trends east-west and is characterized by an Eocene-Oligocene rifting that underwent tectonic inversion during Miocene. It consists of the Sakala High, Kangean High and onshore Madura. The Transitional Terrace is an E-W trend and extends from the Kangean High to the east towards west into Madura Island and the northern tip of East Java Island where it is known as Rembang High. The Southern Basin is filled with thick Miocene and Pliocene sequences and is characterized by a subsidence slow period during Miocene. The Southern Basin is essentially a Miocene Basin.

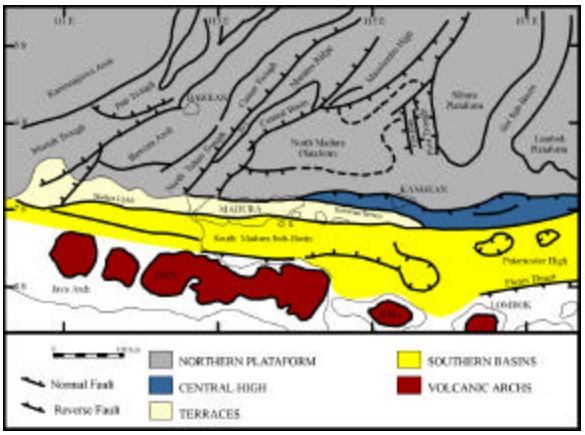

Figura 4: Tectonic provinces onshore East Java and on Northern Platform.

A tensional stress regime was active from the Middle Eocene up to the Early Miocene. The initial stage of extension was marked by rifting during Eocene, followed by a basin-wide subsidence in the Oligocene.

Neogene tectonism is marked by changes of stress regimes in East Java Sea Basin. These lead to widespread inversion during Middle Miocene. Tectonic style changed from quiescent post-rift subsidence to active translation and rotation movements of major fault blocks.

Stratigraphy

Three stratigraphic megasequences are recognized in the seismic lines: (1) Pre-Ngimbang Mgasequence; (2) Paleogene Megasequence and (3) Neogene Megasequence. The Paleogene Megasequence is characterized by sediments filled into rift W-E complex. The Neogene Megasequence is characterized by sediments filled into inverse complex.

The Pre-Ngimbang Megasequence is mud-dominated with lesser siltstone and some sandstone interbeds and rare late Cretaceous marine microfossils. Some well data suggests however that the “Pre-Ngimbang Fm.” may represent a sequence of possible Tertiary age.

Paleogene sediments were deposited within an open marine environment. The Ngimbang Fm. corresponds to the deposition of alluvial/deltaic clastic sediments dated from Early Eocene to Middle Eo-

cene. During Middle Eocene, a wide area was still emergent which provided good source for clastics deposition. The Late Eocene corresponds to the deposition of marine shales and marine carbonate, with possible reef development over previous basement highs on the edges of grabens. Eocene Ngimbang shales are source rocks yielding hydrocarbon ocurrences.

As transgression continued troughout Early Oligocene time, the relief of land masses was greatly reduced. Reef development continued in some areas, although regionally these carbonate sequences gradually become more marly platform deposition. These Late Eocene-Early Oligocene sediments are known as the CD Formation.

During Late Early Oligocene time, the northern part of the Java Sea was uplifted concurrently with a worldwide eustatic sea level fall and the area was flooded by the marine clastics of the Kujung Unit III. In some restricted areas, shallow water limestones continued to be deposited throughout this regressive period. Shales of the Kujung III are within the oil window in many instances.

During Late Oligocene time the area again underwent a transgressive event. Kujung unit II clastics and shalow water limestones were deposited at this time. The Kujung II carbonates are oil and gas reservoirs accumulations northwest of Madura. During Late Oligocene and Early Miocene time, massive limestones of the Kujung Unit I (gas reservoir) developed reefs in areas favourable for their growth.

The Neogene Megasequence during Early Miocene time uplift in Kalimantan led to an influx of fine clastics of the OK Formation. These overlies the Kujung I and provides regional seal. This influx of clastics terminated the Kujung reef growth, except in a few areas (e.g. Rancak Limestone). Transgressive shallow marine deposition resumed during late Middle Miocene through Pliocene time, where it is recorded by fine clastics and carbonates of the Karren Fm. Pliocene and Recent clays complete the overburden (Figure 5).

Seismic Interpretation

Eight seismic horizons representative of structuring were interpreted: (1) Basement; (2) Pre-Ngimbang Fm; (3) Ngimbang Fm; (4) Kujung III Fm; (5) Kujung II Fm; (6) Kujung I Fm; (7) OK Fm and (8) Early Pliocene.

Basement consists essentially of NE-SW trending platform area further north, and an inverted half-graben known as Central Depression towards south. Near the Madura coastline the central trough is bordered by another basement high (Figure 6).

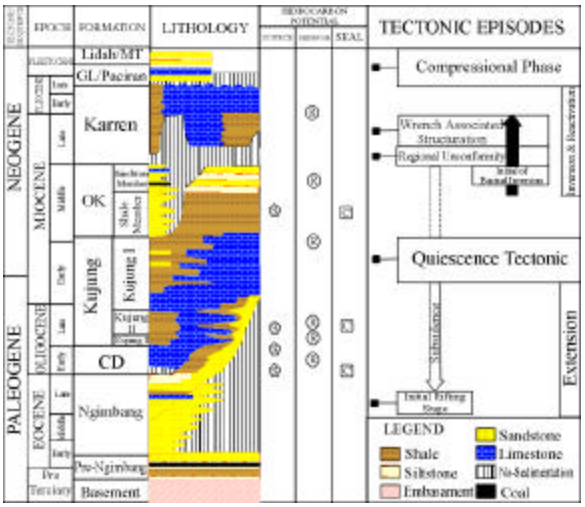

Figure 5: Generalized Stratigraphy of East Java and correspondent tectonic episodes.

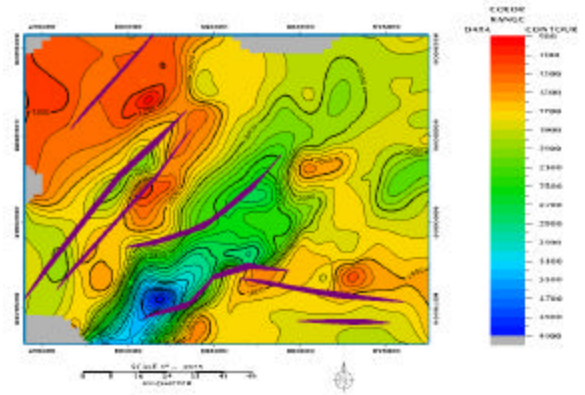
Figure 6: Basament Map.

The main area of inversion trends along a NE-SW direction. All the tectonic provinces of East Java are recognised in the 2D seismic lines. Paleohigh and paleolow structures are distinguished by lithological thinning and thickening over the older Eocene units. Seismic interpretration also revealed the platform areas unaffected by tectonic inversion and the localized half-grabens which were subsequently inverted (Figure 7 and 8).

The Kujung I Fm. marks the seismic boundary between the Paleogene extension and the Neogene inversion. Early Miocene and younger uplifts have affected a large area of the East Java Sea. These uplifts have evolved by reversal movement on normal faults which had previously accomodated Paleogene subsidence. The grabens and half-grabens which existed until early Miocene were inverted and the largest anticlines were generated (Figure 7 and 8).

Three distinct Neogene units are recognized in seismic lines: 1) Early to mid Miocene highstand progradation; 2) Transgressive Late Miocene termi-

nated by Early Pliocene lowstand and 3) Plio-Pleistocene sedimentation.

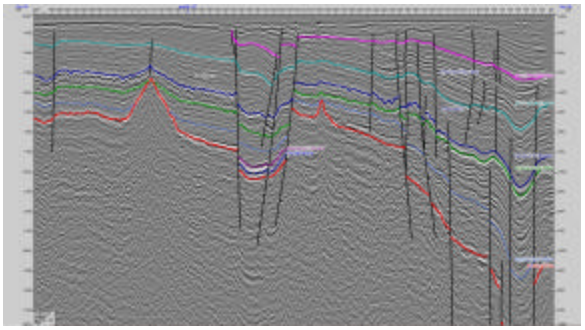

Figure 7: Seismic record gpmi96-103.

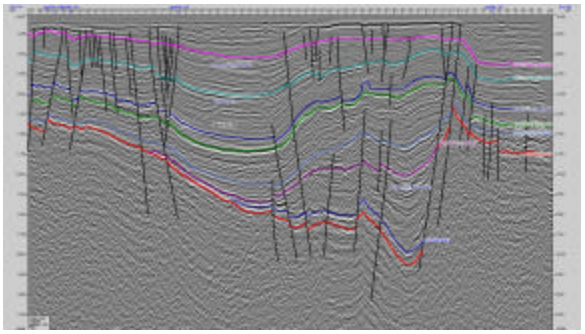

Figure 8: Seismic record gpmi96-104.

Conclusions

The East Java Sea Basin have all tectonic requeriments for hydrocarbon entrapment: source rock kitchens; development of good reservoir and seal facies; and a clear structural distinction between early basement highs and inverted graben structures.

Paleogene tensional stresses led to the development of NE-SW trending tilted horst blocks and grabens. Neogene tectonism related to strike-slip movement led to development of inversion structures and is the major structural control in the region.

The newly acquired non-exclusive seismic survey enabled imaging of deeper beds beneath the carbonates. Seismic interpretation unraveled new exploratory plays: 1) Broad young anticlines of the zones of inversion are attractive Kujung I and II targets (Figure 9); 2) Deeper Eocene Ngimbang plays are yet to be drilled. These consist of structural closures and of stratigraphic wedges onlapping basement.

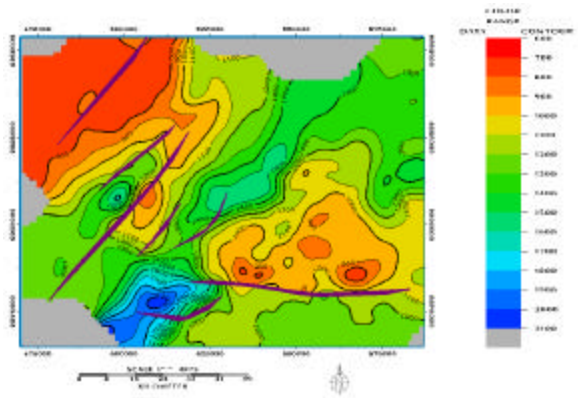

Figure 9: Structural map of Kujung Fm. Carbonates. Several Kujung I and Kujung II prospects are attractive.

References

Ardhana, W. 1993. A Depositional Model For The Early Middle Miocene Ngrayong Formation and Implications For Exploration In The East Java Basin. *Proceedings Of The Indonesian Petroleum Association, 22nd Annual Convention*: 395-443.

Beddoes, L. R. 1981. Hydrocarbon Plays In Tertiary Basins Of Southeast Asia. *Energy*, **6** (11): 1141-1163.

Bransden, P. J. E. & Mattews, S. J. 1992. Structural And Stratigraphic Evolution Of The East Java Sea, Indonesia. *Proceedings Of The Indonesian Petroleum Association, 21st Annual Convention*: 417-453.

Fainstein, R. 1997. Seismic Interpretation Offshore Madura, East Java Sea, Society Exploration Geophysicists, Annual International Meeting, Dallas.

Fainstein, R. & Raharja, M. 1989. Pagerungan Seismic Interpretation. Atlantic Richfield Bali North Publication, 1 (text), 2 (maps) and 3 (seismics).

Hamilton, W. 1979. Tectonics Of The Indonesian Region. US Geological Survey Professional Paper, 1078.

Acknowledgments

We would like to thank Schlumberger WesternGeco for permission to publish this work and Schlumberger GeoQuest for the seismic interpretation softwares.

Volume Interpretation Techniques

Márcio Spínola, Landmark Graphics, Brasil
Carlos Eduardo Abreu, PETROBRAS S/A Brasil

Abstract

Digital Volumetric Images play important role in medical imaging as well in geology and geophysics. In the past recent 6 years advances in computer hardware and software have brought this technology that began to be applied for medical purposes and now is widely available for geoscientists.

This work attempts to discuss volume interpretation techniques of 3D seismic data. The techniques are presented with emphasis on definitions and functionality. Fist we present the volume visualization and interpretation techniques, including color maps, histograms, opacity, attribute analysis, horizon, faults and Voxbody[1] interpretation. Further we present Advanced Volume Interpretation techniques[1], including image processing covering automated volume recognition (*Body Labeling*), morphology operations (*Morphology*), and copy of seismic data using predefined *masks (Shape Cutter*). Together all these tools can be combined to create structural or stratigraphic interpretation workflows. Insights using real data as examples are given.

1. Introduction

Digital Volumetric Images are 3D image arrays corresponding to a stack of two-dimensional slices produced by some scanning technology (Lohmann, 1998). Volumetric images can be generated from many different methods, for instance in computer tomography (based on X-ray beans), magnetic resonance tomography, ultrasound, microscopy, and seismic acquisition and processing. Such images play important role in medical imaging as well as interpretation of geological bodies from 3D seismic volume.

3D seismic volumes are time or depth sequences of 2D images obtained from seismic acquisition and processing. The building blocks of three-dimensional images are *volume elements* or *voxels*[2]. A *voxel*, or volume pixel, is the smallest distinguishable box-shaped part of a three-dimensional image. *Voxels* are used to render seismic attributes like amplitude, acoustic impedance, coherence, etc. For a true 3D image, voxels must undergo opacity transformation. Opacity transformation gives voxels different opacity values. This is important when it is crucial to expose interior details of an image that would otherwise be hidden by darker more opaque outside-layer voxels.
This work attempts to discuss volume visualization and interpretation techniques of 3D seismic data. First we discuss some of most the frequent visualization and volume interpretation techniques including color maps, histograms, opacity, attribute analysis, horizon, faults and *Voxbody*[2] interpretation. Further we present Advanced Volume Interpretation techniques, including image processing derived from medical industry.

2. 3D Visualization Techniques

2.1. Working with synthetics (Tie well to seismic)

One of the essential jobs in volume interpretation is to tie available well information to seismic. This procedure allows geoscientists to make correlation between formation tops interpreted from well logs to the observed seismic, being critical to the quality of interpretation.
Henry (1997) pointed out that without the understanding of wavelet as the filter through which geology is viewed when interpreting image provided by seismic data, there are many equally valid geological interpretations of the actual subsurface geology
The benefits about identify high frequency well information (lithology, markers) on low frequency seismic information (high area coverage) is to provide interpreter key links to identify reservoir facies. Also to it is part of workflow to generate time depth tables that can be used to display well logs in time, build 3D velocity models for posterior conversion of seismic traces from time to depth.

2.2. Color maps and histograms

Once seismic volume is loaded from disk to the computer RAM memory for visualization purposes, interpreters can highlight events on seismic data by simply addressing a color table to a range of attribute values. The objective is to emphasize seismic features that reflect changes in the acoustic property of the rocks (impedance) and may be closely related to lithology changes, facies variation, presence of fluid or gas saturation. Doing so the contrast and visibility of such features are increased.

[1]Some definitions follow the Landmark's volume visualization and interpretation tool EarthCube®
[2] http://www.pcwebopedia.com/TERM/v/voxel.html

Color scales are never the same. Each seismic dataset has different characteristics in terms of attribute distribution (amplitude or acoustic impedance). Histograms computed from seismic data (Figure 1a), changes according to scale applied during data loading operations. Usually seismic data are stored in dynamic range format from 8 to 32 bits. Due memory limitation, a rescale mapping is required for visualization, in such way that histogram distribution, that is function of scaling factor parameter being used, preserves high amplitudes, avoiding spikes at the tails.

For visualization and volume interpretation, we associate a color table to the calculated histogram of seismic data. That means we have one specific color map to express the distribution of seismic attribute. Thus contrast and visibility of lithology variation can be enhanced.

This is a very simple but powerful visualization technique, and usually requires patience in order to come up with a good color map to stress some desired ranges of seismic attribute.

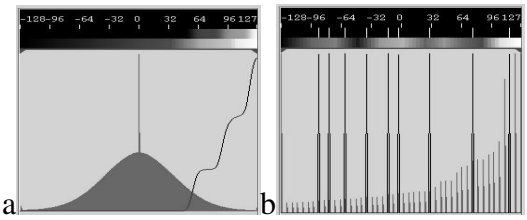

a b

Figure 1 – (a) Histogram, color map and opacity curve used for the visualization of seismic volume displayed in Figure 2. (b) Histogram of *Body Labeling*. Spikes represent detected bodies and associated volume (crescent order from left to right). Note the opacity curve also represented as spikes in order to select prospective bodies. (All figures as courtesy of Landmark Graphics)

2.3. Opacity (Amplitude extremes analysis)

Opacity is a property of materials objects related to the transmissivity of light in itself. We can think opacity in opposite terms: how transparent, for instance, a glass window is regarding the passage of light. Likewise in the virtual world, opacity is a component property used for rendering *voxels*. For a true 3D image, *voxels* must undergo opacity transformation, which gives *voxels* different opacity values. For further readings on how OpenGL blends light and opacity properties to render 3D images in computer, please refer to Woo and Davis (1997).

Opacity is an important visualization technique applied to seismic data. It enables interpreters to examine and comprehend the spatial relationship of seismic anomalies (amplitude or impedance).

By applying an opacity function (or transparency) to a seismic data, we can filter the background noise values and focus on anomalies that could represent geological features (Figure 1).

Since opacity is a pure visualization technique, from a top view perspective of earth model, we are stacking seismic anomalies in different time slices, producing what Bill Keack and Nick Purday call *Optical Stacking*. Optical stacking is an excellent technique to visualize and delineate external geometry of geological bodies (Figure 2). Extreme amplitude values might be associated with zones of interest (carbonate or siliciclastic reservoirs, presence of fluids, etc.).

Opacity leads interpreters to quickly focus on interest areas and furnish straight information on what is good to work on. Usually an amplitude analysis is performed observing how different the external geometry is, regarding opposite attribute values.

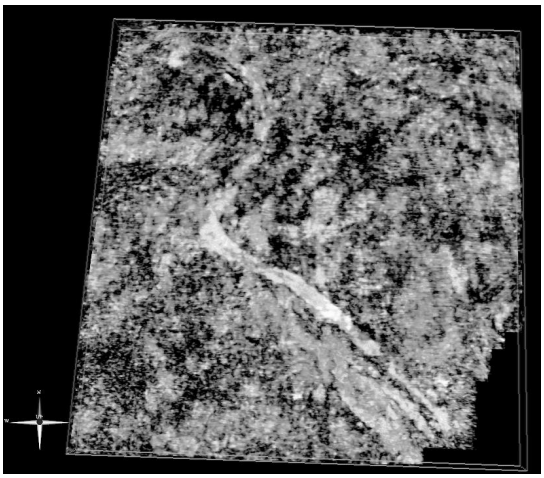

Figure 2. Shows some sand bodies produced from the seismic inversion cube. An opacity curve is also shown with the corresponding histogram of amplitude. Note how extreme amplitude values are distributed in space.

2.4. Horizon and fault interpretation

The interpretation of regional markers defines the structural framework for posterior reservoir modeling. From the seismic data, surface interpretation can be done by manual or automated horizon tracking techniques. One of these techniques is the *opacity tracking*[1].

Opacity tracking enables interpreters to automatically extract horizons from seismic data based on opacity range values within which seed points lies. Tracking can be applied to particular data clusters that repre-

sent extreme continuous coherent reflectors and might (or not) be associated to the reservoir.

Although some problems may occur when no continuous or coherent reflectors associated for instance with erosional unconformities or salt structures are present, generally some regional markers with high impedance contrast can produce extensive horizon picking. They may represent sequence boundaries, for instance, maximum flooding surfaces (MSF). In such cases opacity tracking furnishes enormous advantage over the traditional interpretative workflow done line by line and trace by trace. Even more complex cases can be worked on dividing large areas into small ones and performing a re-tracking when necessary. Here interpreter acts more like a supervisor, worried about QC of the automated interpretation.

Regarding Fault interpretation, Seismic plane animation is a suitable visualization technique to detect and identify faulted zones and how it evolves through volume, appearing or disappearing in different line/traces. Also it is a good method to detect the presence of individual subtle faults.

Fault interpretation task is better accomplished by means of using seismic attributes like coherence cube. When mapped on horizon slices, coherence cube information can provide good insights to correctly position faults. Also coherence volumes can be visualized and interpreted on time slices, seismic planes or horizon slices.

2.5. Attribute analysis

Seismic attributes can be calculated in a time window around interpreted horizon. The result is a map that that can summarize aspects of seismic data within a stratigraphic sequence.

These maps displayed in 3D as overlays on a given horizon, stresses structure and can be combined with different types of information on its real spatial location. It helps interpreter to identify potential areas where better net to gross, gross porosity, presence of channels, lobes, faults, tunning effects are located, acting as guiders for prospect delineation and well path planning.

There is no rule in order to select a particular attribute. It depends on the prospect and the particular interest in study. Some frequent attributes are: RMS amplitude, instantaneous phase, half time energy, total energy, maximum amplitude, etc.

Instantaneous phase can enhance weak coherence events that may be helpful to identify pinchouts, internal depositional geometries, faults pinchouts, oil and gas contact changes, etc (Landmark, 1999). The calculated root mean square attribute (RMS) is sensitive to extreme amplitude values.

2.6. Voxbody and Volumetrics

Once reservoir targets where identified in particular zones, one can isolate different geologic intervals and compute volumetrics through *Voxbody Interpretation*[1]. *Voxbody* consists of a set of connected *voxels*, and can be generated by tracking or sculpting seismic volume.
Tracking consists in selecting parameters like amplitude range, neighborhood criteria and picking a valid seed point (or multiple seed points) from the 3D seismic. Sculpting consists in defining an upper and lower surface (actually could be the same surface shifted in time/depth) and removing the seismic data above and below the bounding intervals. The result is a slab of seismic data that can contain for instance a parasequence.
Formation isolation via sculpting consists in a valuable technique when combined with other visualization techniques like opacity. An optical stacking furnishes much information about geometry and stratigraphy.

3. Advanced Volume Interpretation

Advanced volume interpretation tool include image-processing techniques (from Foster Findley Associates) allowing *voxel* manipulation, automated feature recognition (*Body Labeling*), morphology operations (*Morphology*), seismic volume math (useful for 4D seismic) and copy of seismic data using pre-defined *masks (Shape Cutter*). Together all these tools can be combined to create structural or stratigraphic interpretation workflows.
These tools enhance structural or stratigraphic interpretation workflows, enabling manipulation of multiple seismic attributes that combined with other types of information can be user to infer lithology, stratigraphy and other properties.

3.1. Automated feature recognition (body labeling)

Body labeling[1] allows interpreters to automated extract geological features without seed picking. It consists in defining volumetric criteria for isolating 3D features.
Four parameters are taken into account by the algorithm for accepting or rejecting geological bodies: amplitude range, minimum and maximum number of *voxels* and connectivity. The output produces a set of

bodies sorted according to volume size. Each body contains information about seismic continuity.
Figure 6 shows the results of body labeling run in the same volume as Figure 2. Note that it produces a much clear image. Each detected body produces a spike and an opacity curve can be applied to isolate possible sand bodies (Figure 5). Each continuous individual body receives a label and an associated color (that explains the word *labeling*). Volumetrics then can straight be calculated.

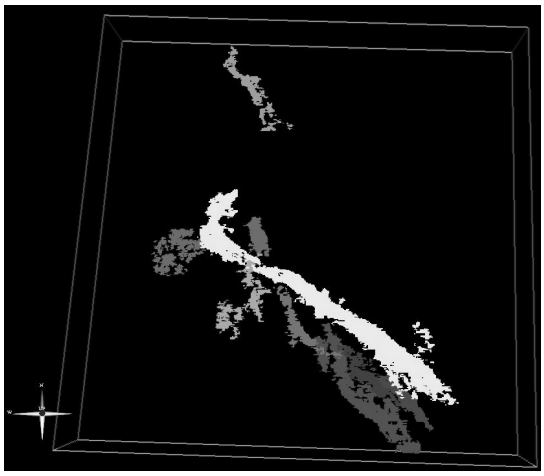

Figure 6. Masks produced by body labeling algorithm. Only prospective bodies are shown.

3.2. Shape cutter

Next step after isolating reservoir bodies would be populating these regions with seismic data (Figure 7). One of the benefits of isolating seismic is working with seismic attributes of the interest zones, for volumetrics computation, horizon interpretation (voxbody wrapping) or body labeling. Later we are going to use this information to guide us in the definition of the planned well targets.

3.3. Morphology

Morphology is frequently used after sub-volume detection. Processing algorithms like Opening or closing can be applied in order to fill out holes or extend volumes beyond detected regions. Further reading about morphology operations can be found in Stoyan *at all* (1995{1985}).

4. Conclusions

We review a set volume visualization and interpretation techniques. All these tools can be used in structural and stratigraphic interpretation workflows to enhance prospect evaluation and characterization. We view volumetric interpretation and visualization as a new form of communication. Also new developments in the hardware and software from universities and industry will greatly impact the reservoir modelling workflow. New virtual reality (VR) application developments will bring new perspectives for the recent future, and the use of gloves for hand picking (instead of mouse picking) and voice recognition are some of the innovative approaches expected for the next years.

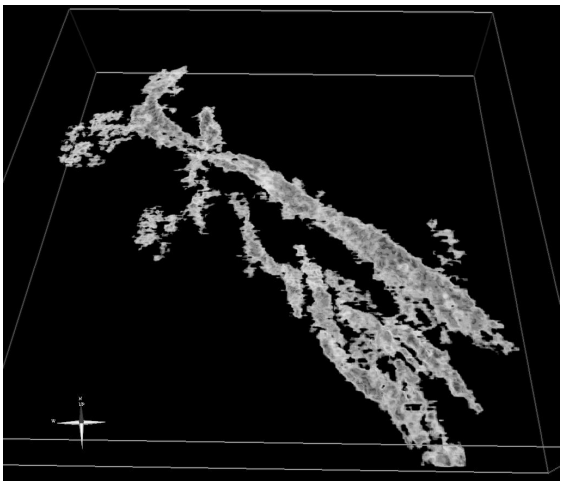

Figure 7. Captured seismic amplitudes of isolated reservoir bodies. Note the presence of channels and associated crevasse splays facies.

References

Keach B, & Purday, N. 2000, Immersive Training Class. September 18-23. Houston – EUA.

Henry S., 2000, Pitfalls in Synthetics. The Leading Edge, June, 604-606.

Lohmann, G., 1998, Volumetric Image Analysis: Wiley & Teubner, 243p.

Landmark, OpenBooks. Postack Family Reference Manual. Marck 1999. Landmark Graphics Corp.

Stoyan, D., Kendall, W. S., Mecke, J.. Stochastic Geometry and its Applications. West Sussex, England: Wiley, 1995{1985}. 436p.

Woo M., Neider, J., Davis T., 1997. OpenGL Programming Guide. Addison-Wesley Developers Press. 2nd Ed. Massachusetts. 650p.

Acknowledgments

We would like to thank PETROBRAS and LANDMARK GRAPHICS for the courtesy to publish this work. We are also grateful to the professionals, Nick Purday, Bill Keach and Yerko Guerra for the useful lessons on volume interpretation.